A Method for Correcting and Reducing the Pressure Data Recorded at the PAM II Stations During GALE

by

Ronald L. Dunic

A thesis submitted to the Graduate Faculty of
North Carolina State University
in partial fulfillment of the
requirements for the Degree of
Master of Science

Department of Marine, Earth, and Atmospheric Sciences

Raleigh

1989

Approved By:

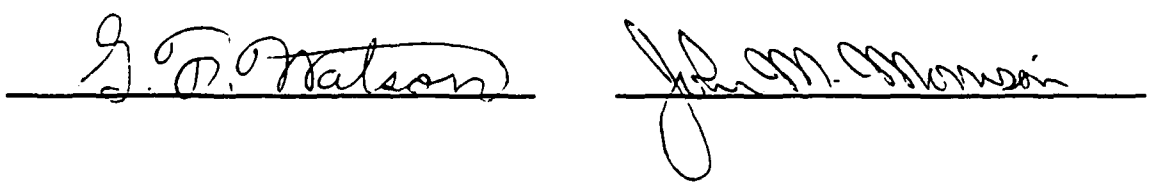

Chairman of Advisory Committee

SECURITY CLASSIFICATION OF THIS PAGE

REPORT DOCUMENTATION PAGE

Form Approved OMB No. 0704-0188

1a. REPORT SECURITY CLASSIFICATION: UNCLASSIFIED	1b. RESTRICTIVE MARKINGS: NONE
2a. SECURITY CLASSIFICATION AUTHORITY	3. DISTRIBUTION/AVAILABILITY OF REPORT: APPROVED FOR PUBLIC RELEASE; DISTRIBUTION UNLIMITED.
2b. DECLASSIFICATION/DOWNGRADING SCHEDULE	
4. PERFORMING ORGANIZATION REPORT NUMBER(S)	5. MONITORING ORGANIZATION REPORT NUMBER(S): AFIT/CI/CIA-89-087
6a. NAME OF PERFORMING ORGANIZATION: AFIT STUDENT AT NC State Univ / 6b. OFFICE SYMBOL (If applicable)	7a. NAME OF MONITORING ORGANIZATION: AFIT/CIA
6c. ADDRESS (City, State, and ZIP Code)	7b. ADDRESS (City, State, and ZIP Code): Wright-Patterson AFB OH 45433-6583
8a. NAME OF FUNDING/SPONSORING ORGANIZATION / 8b. OFFICE SYMBOL (If applicable)	9. PROCUREMENT INSTRUMENT IDENTIFICATION NUMBER
8c. ADDRESS (City, State, and ZIP Code)	10. SOURCE OF FUNDING NUMBERS: PROGRAM ELEMENT NO. / PROJECT NO. / TASK NO / WORK UNIT ACCESSION NO.

11. TITLE (Include Security Classification) (UNCLASSIFIED)
A Method for Correcting and Reducing the Pressure Data Recorded at the PAM II Stations During GALE.

12. PERSONAL AUTHOR(S)
RONALD L. DUNIC

13a. TYPE OF REPORT	13b. TIME COVERED	14. DATE OF REPORT (Year, Month, Day)	15. PAGE COUNT
THESIS/DISSERTATION	FROM _____ TO _____	1989	72

16. SUPPLEMENTARY NOTATION
APPROVED FOR PUBLIC RELEASE IAW AFR 190-1
ERNEST A. HAYGOOD, 1st Lt, USAF
Executive Officer, Civilian Institution Programs

17. COSATI CODES			18. SUBJECT TERMS (Continue on reverse if necessary and identify by block number)
FIELD	GROUP	SUB-GROUP	

19. ABSTRACT (Continue on reverse if necessary and identify by block number)

20. DISTRIBUTION/AVAILABILITY OF ABSTRACT: ☒ UNCLASSIFIED/UNLIMITED ☐ SAME AS RPT. ☐ DTIC USERS	21. ABSTRACT SECURITY CLASSIFICATION: UNCLASSIFIED
22a. NAME OF RESPONSIBLE INDIVIDUAL: ERNEST A. HAYGOOD, 1st Lt, USAF	22b. TELEPHONE (Include Area Code): (513) 255-2259 / 22c. OFFICE SYMBOL: AFIT/CI

DD Form 1473, JUN 86 — Previous editions are obsolete. — SECURITY CLASSIFICATION OF THIS PAGE

AFIT/CI "OVERPRINT"

Abstract

DUNIC, RONALD L. A Method for Correcting and Reducing the Pressure Data Recorded at the PAM II Stations During GALE. (Under the direction of Allen J. Riordan.)

The data recorded at the PAM II stations during GALE will enable researchers to gain a better understanding of the mesoscale processes involved in the various phenomena ~~that occurred during GALE~~; however, the recorded pressure cannot be directly analyzed because it has not been corrected or reduced to sea level. This paper presents a method for correcting the pressure data and then reducing the corrected pressures to sea level.

The Barnes objective analysis scheme was employed to determine the pressure correction for each PAM II station. The corrected pressures are reduced to sea level using the standard NWS reduction procedure outlined in the Manual of Barometry (1963). This method proved to be rather involved and included a number of assumptions to obtain the sea-level pressures. An empirical formula was derived for the GALE dataset to calculate the sea-level pressures for the PAM II stations. Pressure analyses involving the corrected and reduced PAM II pressures for two cases were in good agreement with the NMC analyses for the same times.

Another method for representing the surface geostrophic wind field and the horizontal pressure field, introduced by Pielke and Cram (1987), is explored to determine the true ageostrophic wind components in a cold-air damming situation and to produce a horizontal pressure

field that would eliminate the arbitrariness of the standard pressure reduction procedure. The result is an improvement over the geostrophic wind, but the observed winds are still highly ageostrophic in this cold-air damming situation.

ACKNOWLEDGMENTS

At this time I would like to acknowledge those who contributed to this thesis and express my appreciation. First, I would like to thank the members of my advisory committee: Dr. Allen J. Riordan, the chairman of the committee, for his guidance and editing comments which helped shape this thesis; Dr. Gerald Watson, whose long hours spent programming the Data General enabled me to obtain the results presented in this paper; and Dr. John Morrison, whose comments helped complete this thesis.

Next, I would like to thank the United States Air Force for their financial support and the opportunity to pursue this degree. A thank you also goes out to my fellow graduate students who made sure I did not take the work or myself too seriously.

A special thanks to my parents, Lester and Margaret, and sister, Donna, for the love and support they have given me throughout my life.

Finally, I would like to say a very special thank you to my fiancée, Carole, whose love, support, and understanding helped to preserve my sanity while completing this thesis.

TABLE OF CONTENTS

1. INTRODUCTION

Weather forecasters continue to be frustrated by unforecasted weather events. Every forecaster has experienced the surprise thunderstorm or unexpected intensification of a storm system causing public scrutiny of their forecasting ability. In some cases the result may be nothing more than a picnic being rained out, but in others, property damage and even loss of life may result.

Table 1 shows the spatial and temporal ranges of the synoptic and meso- scales. Synoptic-scale organization has been the basis for much of the success in current weather prediction; however, many damaging or even life-threatening phenomena, such as heatwaves and droughts, arctic outbreaks and heavy snows, flash floods, tornadoes, hail, thunderstorms, windstorms of hurricane force, and downbursts from thunderstorms are all mesoscale phenomena. Many times these events are not predicted because the forecaster is unable to resolve the mesoscale processes involved due to the inability of the current National Weather Service (NWS) surface and upper-air station network to adequately resolve weather systems below the synoptic scale. Thus, the current weather charts do not show everything the forecaster needs to see in order to provide a better prediction.

Another difficulty in forecasting is that the mesoscale processes involved are not well understood. What is needed is a more dense data collection network that would enable forecasters and researchers to identify and study mesoscale features as they develop and propagate to gain a better understanding of the processes at work and subsequently

Table 1. Spatial and temporal ranges for the synoptic and meso- scales (Dirks, et al., 1988).

Scale	Spatial	Temporal
Synoptic	$\geq$ 2000 km	24-48 hrs
Meso-α	200-2000 km	3-24 hrs
Meso-β	20-200 km	$\leq$ 3 hrs
Meso-Γ	2-20 km	$\leq$ 3 hrs

produce a better forecast.

In 1973, the development of a computerized measurement system to be used in the study of a wide range of mesoscale phenomena including hail and thunderstorms, squall lines, sea breezes, and regional air pollution was begun. This system, called Portable Automated Mesonet (PAM), collects and displays mesoscale meteorological data from a surface array of remote sampling systems (Brock and Govind, 1977). The data recorded at the PAM stations include temperature, pressure, humidity, wind speed and direction, and rainfall amounts (Brock and Govind, 1977). This data, when incorporated into the National Weather Service (NWS) station network, enables researchers to study the processes involved in mesoscale storm systems.

The first operational use of a PAM network was during the National Hail Research Experiment (NHRE) conducted in northeast Colorado in 1976. During this experiment, the PAM network demonstrated its ability to "now-cast" surface mesoscale patterns associated with thunderstorm development. The experiment also showed that the PAM network offered researchers a reliable source of continuous mesoscale data as routine

service on the PAM stations was not required (Brock and Govind, 1977).

The Genesis of Atlantic Lows Experiment (GALE) conducted during the winter of 1986 deployed a network of fifty PAM II stations through North and South Carolina and Southern Virginia in order to gather data to enable researchers to study the mesoscale processes associated with East Coast storms. These PAM II stations measured in-situ temperature, wet-bulb temperature, station pressure, wind speed and direction, humidity, dew point temperature, and precipitation amounts.

Of the meteorological data recorded at these and all weather stations around the world, the only parameter that is not directly analyzed is the station pressure. If one constructed a chart with isobars of station pressure, the result would look more like a topographic map rather than a useful weather map because pressure is strongly dependent on elevation. In order to create more useful weather charts, the station pressure is often reduced to a standard reference level to eliminate the effects of elevation on the pressure field and allow forecasters to see the true pressure pattern.

By convention, the reference level chosen is sea level because it is assumed that pressure reduced to sea level will enable forecasters to determine the surface circulation pattern and horizontal pressure-gradient forces (Sangster, 1987). Unfortunately, finding a satisfactory method for reducing the station pressures to sea level has not proven to be an easy task for meteorologists over the past century. The difficulty has involved finding a representative way of depicting

the temperature of the fictitious column of air between the station elevation and sea level.

Due to the concentrated network used during GALE, the pressure data recorded at the PAM II stations may permit a true mesoscale definition of the pressure gradient. From the pressure-gradient field the horizontal pressure-gradient force and the geostrophic wind can be uniquely determined. However, before the PAM II data can be reduced to sea level the data must first be corrected to enable the PAM II network to fit into the NWS station network.

The research described in this thesis deals primarily with enabling the pressure data recorded at the PAM II stations to be incorporated into mesoscale analyses and studying a method of better representing a surface pressure field from which surface geostrophic winds can be computed.

1.1 Literature Review

In order for the PAM II data to be utilized in resolving the mesoscale features, it is important for the data to be meteorologically real and not artificially induced by sensor or measurement errors (Wade, 1987). One method for checking data quality is to use reference sensors transported to each site as was done during GALE. The method provides a useful check on the accuracy of the sensors as long as the calibration of the reference sensors is maintained and a sufficient number of checks are accomplished so as to provide a statistically significant correction (Pike, 1985). Due to the remoteness of some of the PAM II stations, there was not a sufficient number of checks during

the GALE Project.

The errors commonly observed in mesonet data can result from failure of a component in the system, calibration errors, sensor drift, exposure of sensor to the elements, or system noise (Wade, 1987). The detection of these errors requires documentation of the sensor's performance compared with other sensors in the network. This can be accomplished through a direct one-to-one comparison with other stations or through an objective analysis (Wade, 1987). In this research, buddy checks, comparisons between two nearby stations, were performed with a handful of PAM II stations and their nearest NWS station to determine the feasibility of employing an objective analysis to obtain the corrections. As was done in the quality control approach of Wade (1987) this research employs the Barnes objective analysis scheme to obtain the corrections to the PAM II pressure data.

In addition to sensor error, the offsets obtained from the Barnes analysis and buddy check methods are influenced by real sub-grid scale events such as thunderstorms. For the most part these sub-grid scale events are short-lived and the variability, or noise, caused by these events is smoothed by averaging over a number of cases.

Once the pressure data have been corrected, a method of reducing these corrected pressures to a common reference level, usually sea level, can be found. As was stated earlier, this has not proven to be an easy task. During the first thirty years of its existence, the Weather Service used no fewer than six different methods for the reduction of pressure to sea level, with each method improving upon its

predecessor until the Weather Service was confident it had found a useful algorithm. A historical review of the early methods and the problems associated with them is provided in Appendix 8.1.

The Weather Service adopted, and currently uses, a method that includes the work done by Ferrel (1886) and Bigelow (1900). The pressure reduction is accomplished using the hypsometric equation with the temperature replaced by the mean virtual temperature of a fictitious air column representing conditions between the station and sea level. The calculation of the mean virtual temperature includes computation of : (1) the temperature argument defined by Bigelow (1900) as the average of the current temperature and the temperature recorded twelve hours earlier, (2) a standard lapse rate correction, (3) a humidity correction first introduced by Bigelow (1900), and (4) a plateau correction developed by Ferrel (1886) (Manual of Barometry, 1963).

Even with the corrections made by Ferrel and Bigelow, the National Weather Service pressure-reduction method still includes errors that result from the estimation of a lapse rate through the plateau or mountain.

Bellamy (1945) attempted to mitigate the problem of estimating a lapse rate in developing his altimeter correction system because the altimeter equation assumes a standard lapse rate. The obvious problem with this is that the atmosphere seldom follows the standard lapse rate.

To sidestep the sea-level reduction difficulties, Sangster (1960)

devised a method for directly computing the horizontal-pressure gradient force (HPGF) at the earth's surface using station pressures and surface virtual temperatures. The method employs Bellamy's altimeter correction system in order to rewrite the hydrostatic equation, a σ-coordinate system developed by Phillips (1957) where the vertical coordinate is defined by pressure with the surface pressure used as the lower boundary (σ=1 at the surface), a smoothed terrain and finite differences to produce stream and potential functions of the surface geostrophic wind (Sangster, 1960).

In his case studies, Sangster found the geostrophic wind to be less when computed from the streamfunction and potential function charts than when computed from the sea-level charts (Sangster, 1960). He also found evidence that the observed winds are not as ageostrophic as the sea-level isobars would indicate. These two findings result from the potential function, or divergent part of the geostrophic wind. In isobaric coordinates, this divergent part of the wind is zero, but since the sigma-coordinate system is being used, there is a divergence of the geostrophic wind and thus a need for a potential function (Sangster, 1987). Sangster's case studies show that this potential function can yield a component in almost the exact opposite direction as that given by the streamfunction in some locations, thus illustrating that this potential function is not negligible (Sangster, 1987).

Another method for deriving a pressure field and subsequent geostrophic wind field for flat terrain was developed by Pielke and

Cram (1987). Using a terrain following coordinate system derived by Pielke and Martin (1981) and the slope-flow equations developed by Pielke et al (1985), Pielke and Cram redefine the geostrophic wind equations where the pressure-gradient term is the sum of the modified pressure gradient along a σ-surface and terrain-gradient terms. This method derives a flat-ground surface-pressure field which is consistent in concept with the currently applied mean sea level (MSL) analyses, but which reduces the apparently excessive pressure gradients that result from conventional MSL procedures (Pielke and Cram, 1987).

Both Sangster and Pielke and Cram seem to have circumvented the difficulty of finding a temperature for a fictitious column of air. The question is which method should be employed. Davies-Jones (1988) compares both methods and concludes that both methods are equivalent. Davies-Jones also concludes that Sangster's method with its use of the altimeter correction system and introduction of a horizontally varying reference atmosphere is more complicated than the method devised by Pielke and Cram (Davies-Jones, 1988). It is for this reason that this research will employ the Pielke and Cram method for determining horizontal pressure gradient over flat terrain.

1.2 Research Goals

The goals of this research are to use the data collected during the Genesis of Atlantic Lows Experiment (GALE) to:

(i) Determine corrections to the pressure data recorded at the Portable Automated Mesonet II (PAM II) stations.

(ii) Determine a method of reducing the corrected PAM II station

pressures to sea level in order to enable the PAM II pressure data to be used in mesoscale analyses.

(iii) Study methods to produce a meaningful surface-pressure field from which to compute surface geostrophic winds, and to determine the true ageostrophic components of the winds during cold-air damming situations.

1.3 GALE Project

The field phase of the GALE project was conducted from 15 January to 15 March 1986. Some of the objectives of GALE (Dirks et al., 1988) were to:

(i) describe the airflow, mass, and moisture fields in East Coast winter storms with special emphasis on mesoscale processes.

(ii) understand the physical mechanisms controlling the formation and rapid development of East Coast storms.

(iii) apply conceptual models and enhanced mesoscale data to the short range forecasting of significant weather.

To accomplish these objectives, analysis of mesoscale pressure fields is vital. A number of mesoscale phenomena and mesoscale processes are associated with East Coast storms and their roles in cyclogenesis needs to be studied (Dirks et al., 1988). Observations from the PAM II stations and near-shore buoys help to spatially resolve borderline meso-α and meso-β scale features. The 5-minute data recorded at the PAM II sites permit the detection of small meso-β and large meso-Γ scale features and enable their observation for periods of approximately twelve hours (GALE, 1985).

2. CASE STUDY DATA AND METHODOLOGY

2.1 DATA

The data for this research are a combination of standard hourly observations at National Weather Service (NWS), Federal Aviation Administration (FAA), and US military stations and special observations at selected sites operated specifically for the GALE field program. This section concentrates on the special observing facilities used in this research.

The objectives of GALE require meso- and even microscale analysis, so the data collection network was intensive. There are two data-gathering areas of particular significance to the present research:

i) Inner GALE Area

In this area, the meso-β processes of frontogenesis and cyclogenesis can be examined. The inner GALE area was approximately 500 km wide, centered on the coast, and extended 1000 km from Georgia to Virginia (Figure 2.1). Portable-Automated-Mesonet (PAM II), Doppler radars, ships, buoys, most aircraft flights and the Cross-chain Loran Atmospheric Sounding System (CLASS) rawinsonde sites were located in this area.

ii) Regional GALE Area

The regional GALE area was 1000 km wide (from the Appalachian Mountains to 500 km offshore), and 1500 km long (from Florida to New Jersey; see Figure 2.1). The regional area will allow meso-α processes of frontogenesis and cyclogenesis to be examined.

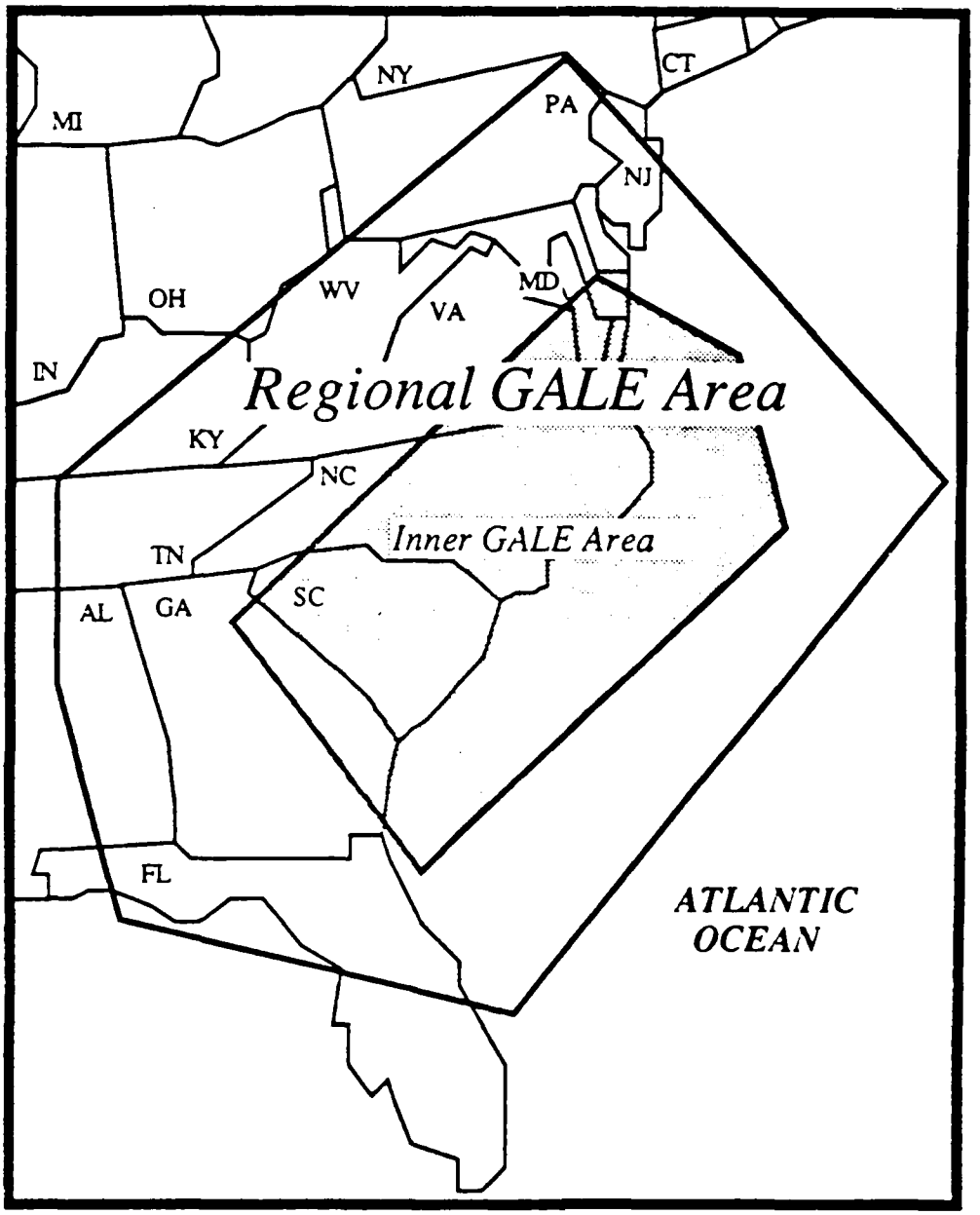

Figure 2.1 This figure shows the locations of the Inner GALE Area (shaded region) and the Regional GALE Area.

2.1.1 Surface Measurements

The surface measurements were designed to provide surface data fields of standard meteorological parameters within the Inner GALE Area with mesoscale resolution and to provide a complement to the data gathered through sounding operations. Standard measurements included air temperature, dew point temperature, barometric pressure, wind speed and wind direction. In addition, land-based stations measured precipitation and sea-based stations measured sea temperature.

The fifty-station PAM II network (Figure 2.2) provided automated 5-minute averaged meteorological surface observations over the eastern half of North Carolina, all of South Carolina, and southeastern Virginia. A line of four stations extended northwestward to support a sounding cross-section for cold-wedge studies.

Deployment of the eight special GALE buoys, including six North Carolina State University buoys and two NOAA-E buoys (Figure 2.2), supported studies of the development of the coastal front and augmented observations in the data-sparse region in the Inner GALE Area.

2.1.2 Ships

The oceanographic research vessels R/V Cape Hatteras (RVC) and the R/V Endeavor (RVE) (the R/V Endeavor participated only in January) operated off the coast of North and South Carolina. The data recorded included wind speed and direction, air temperature, sea-surface temperature, barometric pressure, and humidity. The two ships also served as launch platforms for soundings.

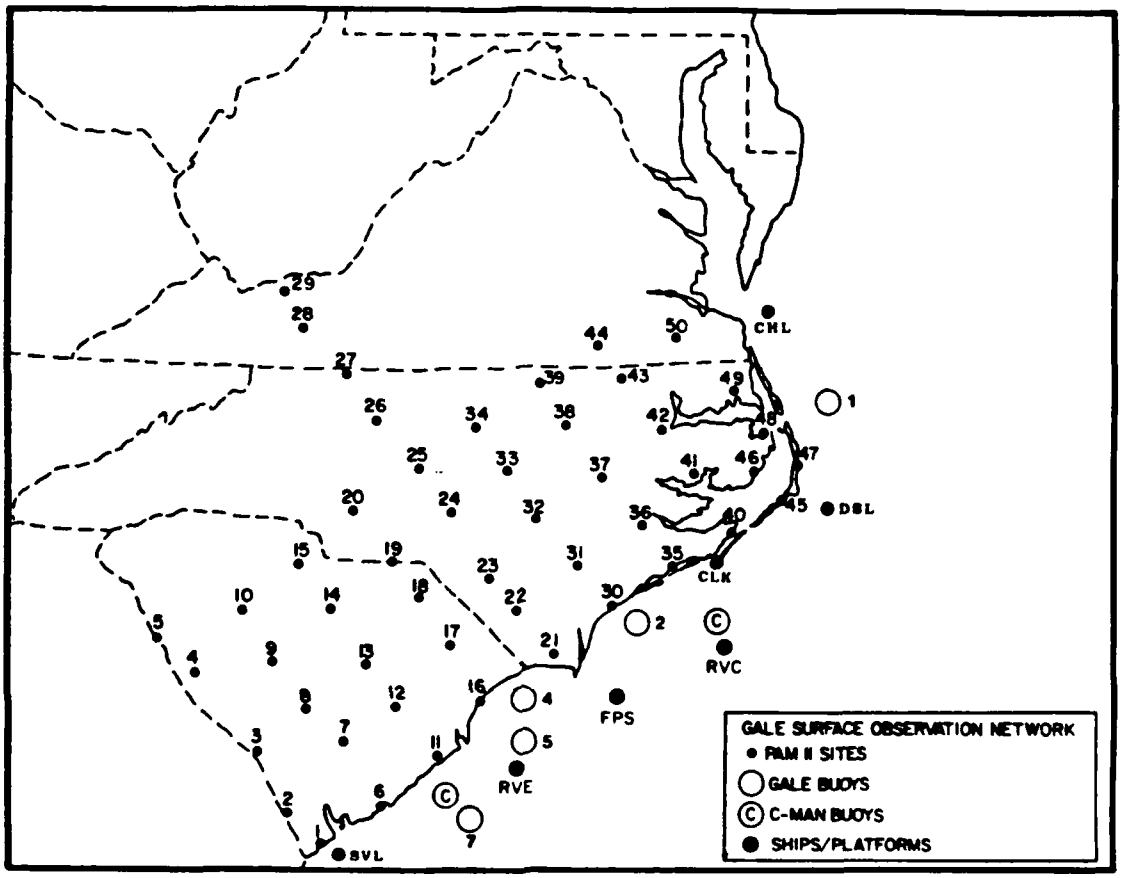

Figure 2.2. Map showing the locations of the PAM II stations and marine buoys, ships , and platforms.

2.2 Barnes Objective Analysis Scheme

The calculation of the pressure corrections and the geostrophic wind fields for this study is aided by the Barnes (1964, 1973) objective analysis method. The Barnes objective analysis scheme is chosen because of its simplicity, accuracy, cost effectiveness, and its several advantages over other similar techniques. From Harms (1985) the advantages of the Barnes scheme are:

i) The scheme is computationally simple and assigns weights solely as a function of distance between datum and grid point.

ii) The weight parameter, which determines the degree of smoothing, can be chosen prior to the analysis so that the pattern resolvable by the data distribution will be revealed.

iii) Since the weighting function approaches zero asymptotically with distance, the influence of data may be extended any distance to insure that a sufficient number of observations influence each grid point without changing the weight function and , therefore, the response characteristics.

iv) Only two passes through the data are needed to achieve the desired pattern.

v) "Noise" is adequately filtered from the analysis so further smoothing by application of additional numerical filters is not necessary.

The Barnes objective analysis scheme accepts data from observation points and mathematically interpolates values to a two-dimensional grid array. The values at the grid points can be used to interpolate data

to station locations such as was done in the pressure correction procedure or be used in finite difference calculations such as in calculating the geostrophic wind components. An additional modification to the scheme was employed in determining the pressure corrections enabling the program to interpolate back to the individual PAM II locations. For example, if q represents any meteorological variable, the interpolated value is just the weighted mean (q) of observations surrounding the grid point. That is,

$$q = \frac{\sum_{i=1}^{n} (w_i q_i)}{\sum_{i=1}^{n} w_i} \qquad (2.1)$$

where n is the total number of stations influencing a given grid point and w is the observation weight.

The observation weights are assigned to the data as a known function of distance between the data and grid points according to

$$w = \exp(-d^2/k) \qquad (2.2)$$

where k is the weight parameter that controls the rate at which the weight value decreases outward from the point of interpolation. Hence, k determines the degree of smoothing of the data field. If k is small, there is little smoothing; if k is large, there is greater smoothing.

The selection of k is important in determining the detail remaining in the interpolated field. The choice of this parameter

value must strike a balance between retaining as much detail as the observation network-density allows and filtering out sources of random and sub-scale error. Structural detail is limited by the minimum resolvable wavelength which is usually twice the station spacing. The GALE PAM II stations have a mean station spacing of about 68 km, while the upper air stations of the Inner GALE sounding (including National Weather Service and CLASS) network have an average station spacing of about 180 km. These distances are about one-half those of the normal operational reporting networks. Thus, theoretically, the Inner GALE networks can resolve features of twice the respective mean station separations, or about 140 km at the surface and 360 km aloft.

The weight parameter, k, is selected to determine the percentage of the amplitudes of the minimally-resolved waves that will be conserved (Harms, 1985). The specific k values used in this application suppress the amplitudes of the two-station-spacing waves to only 16 percent of their original amplitude in the belief that error does make a significant contribution to the amplitudes of the higher frequency features. Sources of "error" include biases introduced by local topography and obstacles at observation sites, features on scales smaller than the station spacing (for example, gravity waves), and turbulent fluctuations with periods of several minutes (especially near the ground). Specific applications of the Barnes analysis scheme will be described in later sections.

3. PRESSURE CORRECTION AND REDUCTION TO SEA LEVEL

The data recorded at the PAM II sites will enable researchers to gain a better understanding of the mesoscale processes involved in East Coast winter storms. A problem with the PAM II data is that the recorded pressure has not been corrected or reduced to a horizontal reference level and, as a result, cannot be used directly to perform mesoscale analyses. This section first presents one method of finding pressure corrections for each PAM II station and then describes a method for reducing these corrected pressures to sea level.

3.1 Pressure Correction

Correction of PAM II station pressures involves a series of steps. First, buddy checks were performed between altimeter settings at selected PAM II sites and nearby NWS stations. Second, time series plots of altimeter differences for each selected station pair were evaluated in order to identify trends. Third, and finally, an objective analysis based only on the NWS altimeter settings was employed to determine the corrections for all PAM II stations.

Initially five comparisons between the calculated altimeter settings of PAM II and NWS stations were made for 24 January, 24-25 February, and 8 March using PAM II sites 3, 9, 26, 33, 34 and NWS stations AGS, CAE, GSO, and RDU. No long-term time trends in the differences were found for these three periods, so the study was expanded to include the entire GALE period.

Buddy checks were performed for the entire GALE period between

each of ten PAM II stations and its nearest NWS neighbor using a calculated altimeter setting for each station. The altimeter setting was chosen in order to reduce the pressure offsets due to elevation differences between the station pairs. The equation used to calculate the altimeter setting is taken from the Smithsonian Meteorological Tables (List, 1966) and is shown below:

$$Alstg_{mb}=(p_{mb}-0.3)[1+(ap_0^n/T_0)(H/(p_{mb}-0.3)^n)]^{1/n}, \quad (3.1)$$

where: $Alstg_{mb}$ = altimeter setting in mb,

p_{mb} = station pressure in mb,

p_0 = standard sea level pressure = 1013.25 mb,

a = lapse rate in standard atmosphere = 0.0065°C/m,

T_0 = standard sea level temperature = 288 K,

H = station elevation in meters,

n = aR = 0.190284, where R is the dry-air gas constant.

Table 3.1 shows the results of the station comparisons over the entire GALE period.

In order to determine how much accuracy could be expected for any given PAM II barometer, the NCAR field calibration checks for the pressure sensors were examined. During field calibrations, teams transported a barometer calibrated at the nearest National Weather Station to a nearby PAM II site and compared the two instruments. Each PAM II barometer was checked at least two and at most five times during GALE. Most of the sites had at least three field calibration checks

Table 3.1. Station Comparisons with the distance between stations in km, and average altimeter difference, standard deviation, and range in millibars.

STATION COMPARISONS

NWS	PAM	DISTANCE (KM)	DIFFERENCE (MB)	STD DEV (MB)	RANGE (MB)
SAV	01	25	0.281	0.378	-1.02 TO 1.41
AGS	03	57	-0.837	0.686	-2.95 TO 1.03
CHS	06	35	0.544	0.599	-2.54 TO 2.86
CAE	09	20	-1.340	0.458	-2.51 TO 0.10
CLT	15	54	-1.045	0.726	-0.72 TO 2.48
ILM	21	50	2.309	0.705	0.61 TO 4.33
GSO	26	25	-0.649	1.003	-4.08 TO 2.25
RDU	33	29	1.763	0.448	0.48 TO 3.35
RDU	34	33	1.188	1.194	-0.51 TO 2.81
GSO	34	75	-0.098	1.355	-3.67 TO 2.81
HAT	45	13	-0.907	0.475	-4.39 TO 0.60

performed during the GALE period.

The field calibration data were not directly used to correct the PAM II station pressures because, as Wade (1985) states, the direct comparison with reference sensors provides a check of the absolute accuracy of the mesonet sensors, but the detection of errors in the data involves the comparison with similar sensors in the network. In other words, in order to fit the mesonet into the existing NWS network, the mesonet sensors must be compared with the surrounding NWS stations to check for errors.

Since it is difficult to obtain a reliable statistic for any given site based on the few comparisons performed per station, all of the comparisons for all sites were combined as follows: An average field

calibration difference was calculated for each site. Then, using this average, an absolute deviation from the mean difference was calculated for each calibration time for each station. These deviations were averaged over the entire PAM II network to obtain an average deviation for the entire network of 0.375 mb, which represents a measure of the absolute resolution of the PAM II sensors. Comparing this with the average differences in Table 3.1 indicates that most of the stations can be improved.

The next step was to plot the altimeter differences over time to evaluate the trends. Over the sixty-day period, the differences show variations of +/- 0.5 to 1.0 mb over the synoptic 2 to 7 day period, and occasional sharp +/- 1 to 2 mb variations over 2- to 3- hour periods.

Comparison with daily sea-level pressure analyses shows that, generally, the differences remain fairly well-behaved during high pressure situations while extended deviations from the mean occur during periods when low-pressure systems are in the area. The magnitude of the differences depends on the orientation of the PAM/NWS pair with the pressure gradient. For example, if the pressure gradient was oriented north-south, two stations oriented east-west would have smaller differences than two stations oriented north-south.

Figure 3.1 shows an example of the synoptic variations. In this figure, the differences fall below the mean (0.281 mb) around 0000 UTC on 19 January and remain below the mean until around 1200 UTC on 21 January. During this time, a low pressure center formed north of the

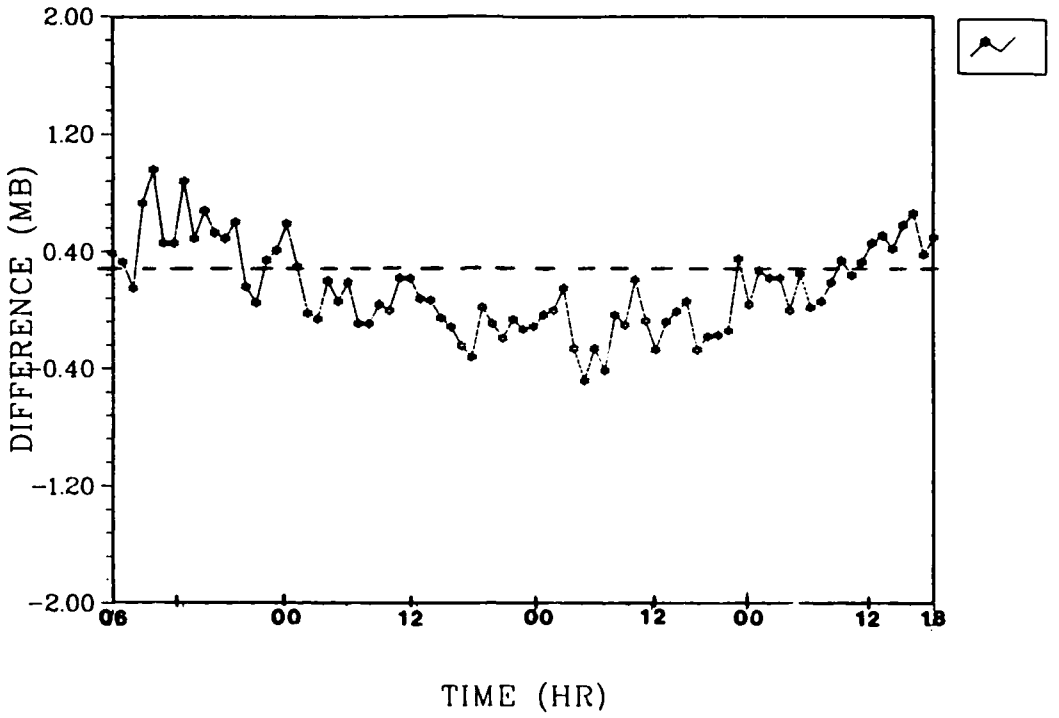

Figure 3.1 Plot of the altimeter difference between Savannah, GA (SAV) and PAM II Station #01 with time for the period 0600 UTC on 18 January 1986 to 1800 UTC on 21 January 1986.

inner GALE region and a persistent surface trough was located west of SAV.

Attention is now turned to the short period variations to determine if they could be eliminated from the data set. Figure 3.2 is a good example of a short period deviation. The differences sharply decrease from 1600 UTC 6 February to a low of -1.50 mb at 1800 UTC on 6 February and return to the mean two hours later. Figure 3.3, showing the altimeter settings for both SAV and PAM II station #01, helps to explain this spike. The sharp decrease in the difference is a result

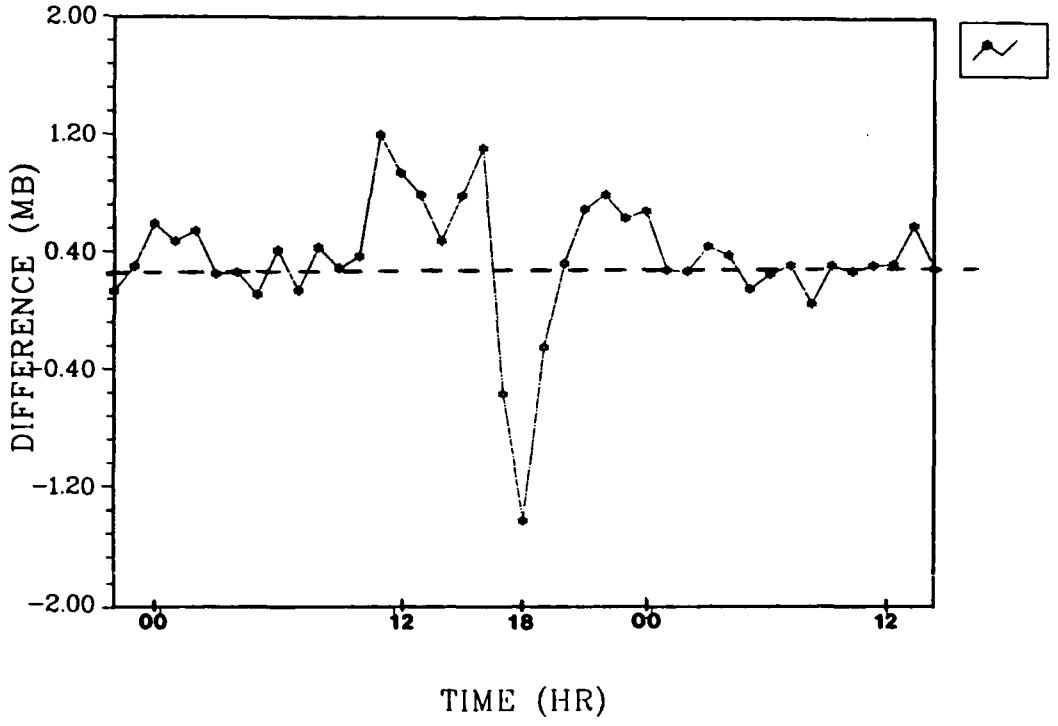

Figure 3.2 Same as Figure 3.1 except for the period 2200 UTC on 5 February 1986 to 1400 UTC on 7 February 1986.

of a temporary rise in the altimeter setting at SAV while the altimeter setting at the PAM II station continued to drop. A frontal system approaching from the west would explain the continued drop in altimeter setting, but a check of the observations at SAV reveals that a thunderstorm was observed at 1610 UTC, lasting for about forty minutes. The resulting mesohigh lasted for two observations (1700 UTC and 1800 UTC) before moving off and allowing the pressure to fall rapidly as the frontal system approached. Therefore, the spike depicted in Figure 3.2 is likely the result of a real small-scale feature and thus it can not be eliminated from the data set. The other spikes in the altimeter

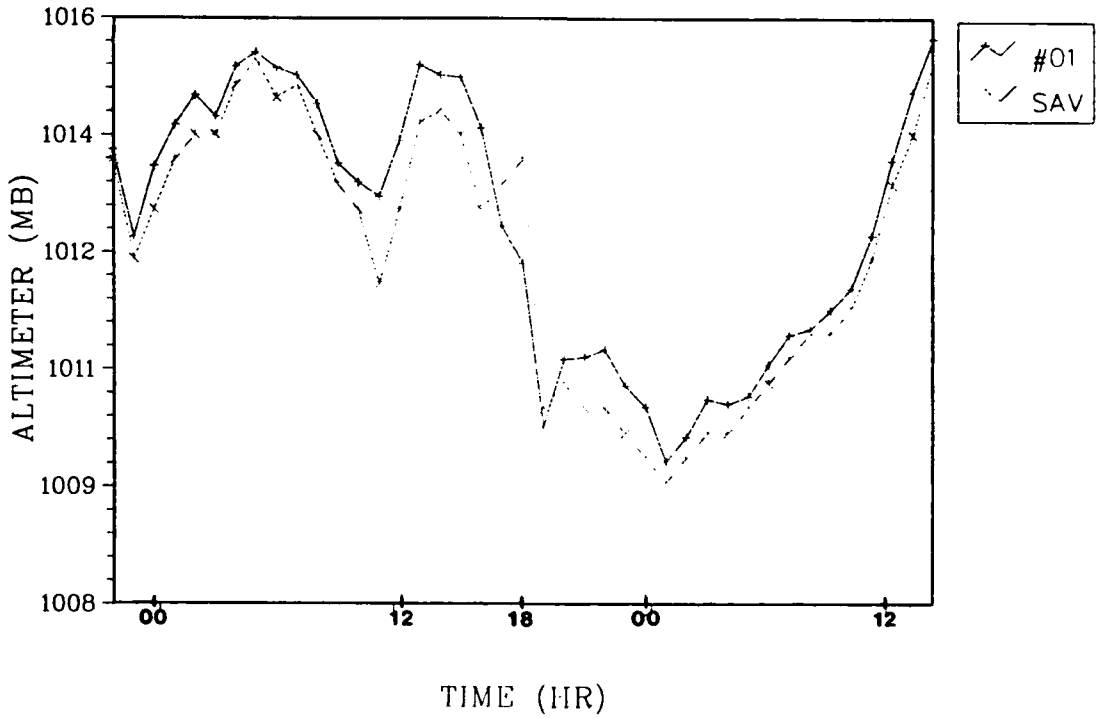

Figure 3.3. Plot of the Altimeter Settings for SAV and PAM II station #01 from 2200 UTC on 5 February 1986 to 1400 UTC on 7 February 1986.

difference plot are, as in Figure 3.2, not usually composed of isolated points so it was decided to retain all of the field data.

Since not all PAM II sites are located near NWS stations, the final step in the correction process involves performing an objective analysis on a field of NWS, FAA, military, and marine altimeter settings to obtain corrections for each station.

A map showing the PAM II sites and the NWS, FAA, military, and marine stations used in the Barnes objective analysis is shown in Figure 3.4. The twelve marine observations help to define the pressure field over the nearby waters. Data from nearshore buoys were

eliminated because, during the data reduction and calibration phase of GALE, the NCSU buoys were found to not be as reliable as expected due to unpredictable drift in calibration. This elimination left only the twelve stations shown in Figure 3.4. Since the height of these marine observations is taken as zero, Equation (3.1) reduces to:

$$\text{Alstg}_{mb} = (p_{mb} - 0.3). \quad (3.2)$$

The cases chosen for analysis have a variety of pressure gradients in order to obtain a better representation of the entire GALE period. Five cases (24 January, 14 and 23 February, and 1 and 8 March) are characterized by small gradients, three cases (2, 13, and 25 February) have a moderate gradient, two (20 January and 6 March) have a strong gradient, and three cases (11 and 27 February and 13 March) have low pressure systems in the GALE region. Thirteen cases were selected so that there would be at least nine offset values for each PAM II site which would then be averaged to obtain the correction for each station.

The 1200 UTC hour was chosen to be used in each case because it is a synoptic hour when a sufficient amount of NWS and marine data are available to perform the Barnes analysis. Furthermore, in order to check the consistency of the Barnes analysis program, the program was run on data for five consecutive hours starting at 1000 UTC on 14 February.

A check was performed before applying the Barnes analysis scheme in order to identify any bogus data. The altimeter settings of each station were plotted for each case. Upon examination of the resulting

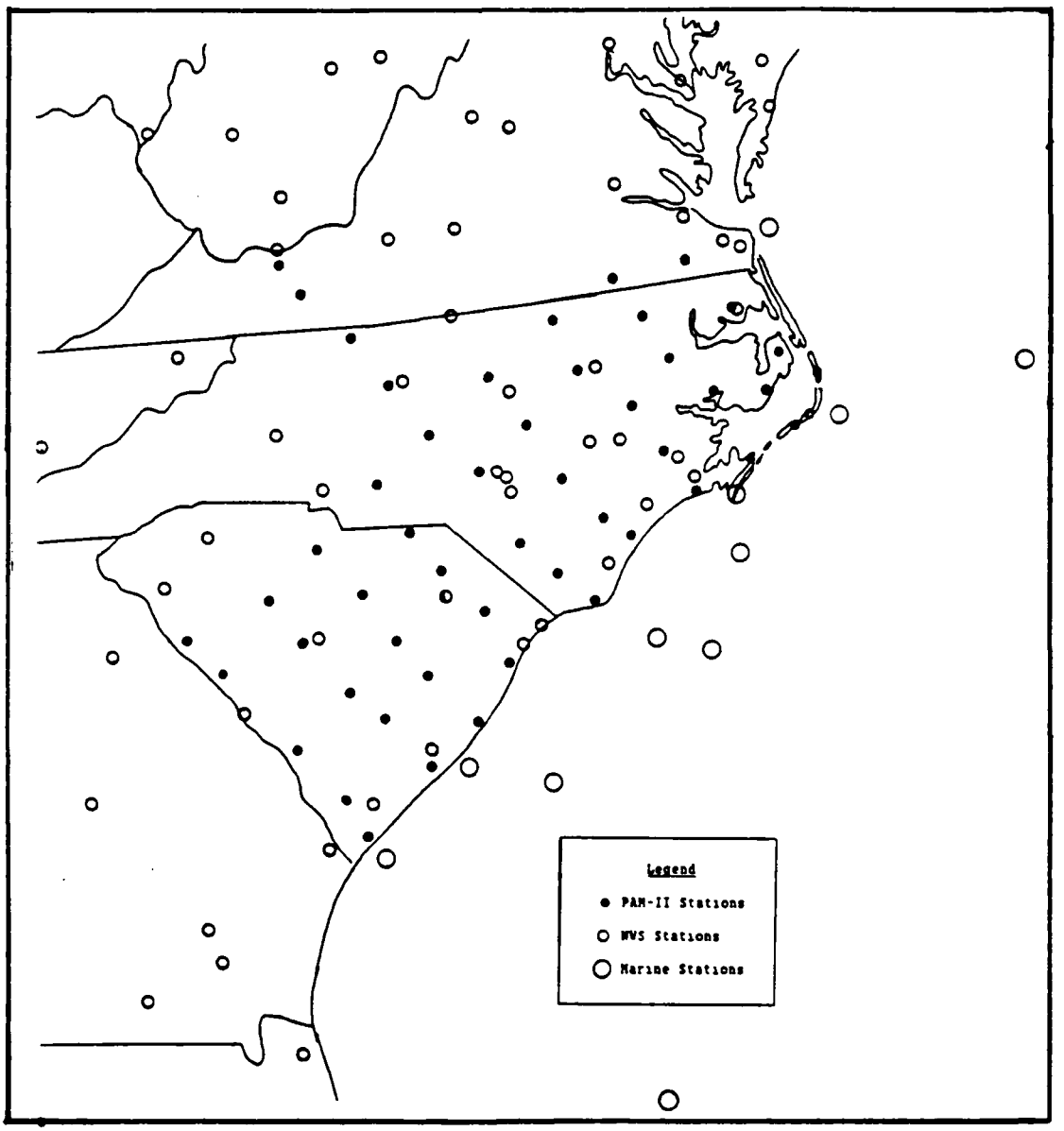

Figure 3.4. Map showing the surface stations employed in the Barnes Objective Analysis Scheme. The PAM II stations are included as a reference.

altimeter field, the altimeter settings at the military stations NBC, NCA, and NKT were found to be consistently lower than the surrounding stations. As a result, these three stations were removed from the data set used by the Barnes analysis scheme.

The Barnes analysis scheme was then applied to the remaining surface NWS, FAA, military, and marine stations. The mean station spacing for this network is about 130 km. Thus, it follows that the minimum resolvable waves are those of 260 km wavelength. A corresponding weight parameter, k, of 10^4 km^2 is used to suppress these minimum resolvable waves to about 16 percent of their initial amplitude at the end of the second pass of the scheme. In order to ensure convergence of the scheme after two passes, a convergence parameter (Γ) of 0.3 is used. Altimeter settings are interpolated to a two-dimensional array of grid points with a mean station spacing of 40 km at 60°N or about 34 km at the PAM II network latitude.

After the second pass of the Barnes scheme, an altimeter setting resulted at each grid point as shown in Figure 3.5. In order to determine the altimeter setting at each PAM II station, another interpolation was done using the data from the four surrounding grid points. This interpolation was accomplished by bilinear interpolation from the surrounding grid points.

Once an altimeter setting was obtained for each PAM II site, the program compared this altimeter setting with an altimeter setting calculated from the PAM II height and raw station pressure data using equation (3.1). An offset was calculated between the interpolated and

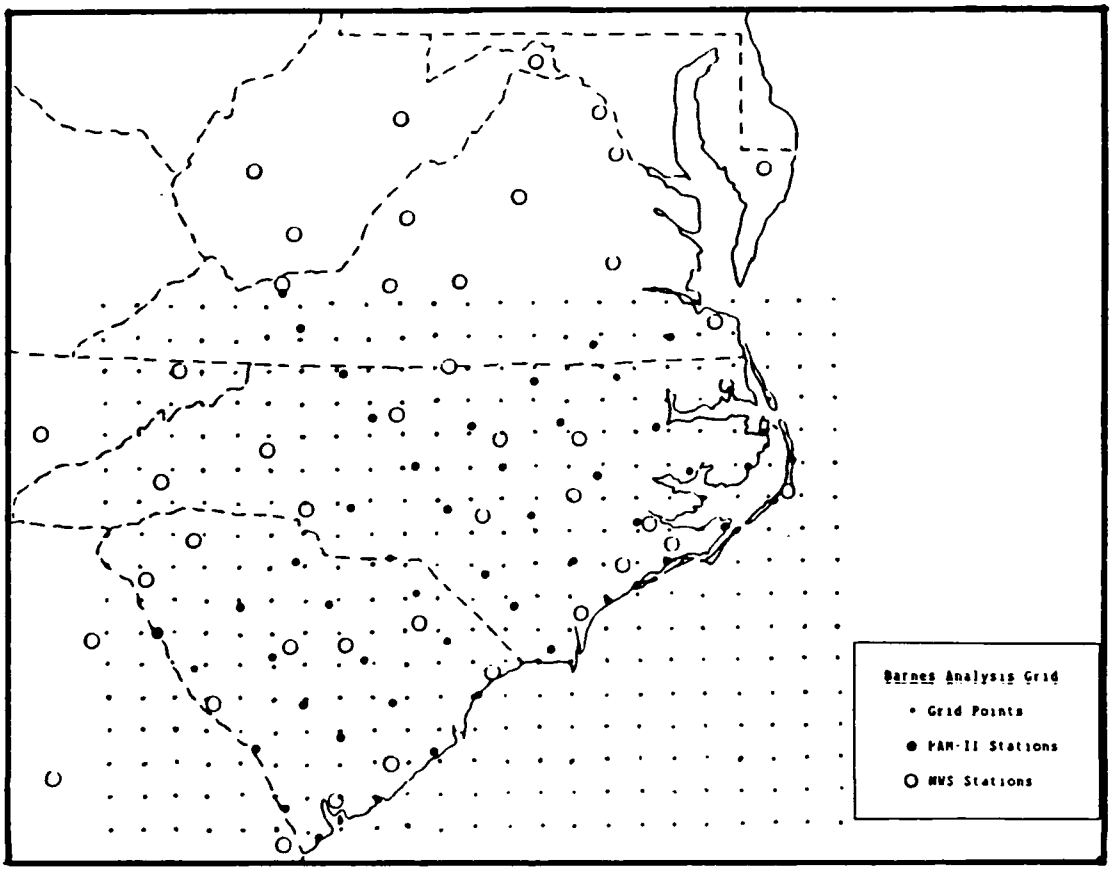

Figure 3.5. Map showing the array of grid points used in the Barnes analysis scheme.

observed values by using the following equation:

$$DIFF = ALSTG_{ob} - ALSTG_{int}. \qquad (3.3)$$

The results for the thirteen cases are shown in Table 3.2 and the results of the five consecutive hours are shown in Table 3.3.

From Table 3.3, the corrections obtained from the Barnes scheme for nearly all stations during the five consecutive hours range within +/- 0.375 mb, which was previously determined from the field calibration data to be the resolution of the PAM II instruments.

Table 3.2. This table shows the results of the Barnes objective analysis. Units for the average differences and standard deviation of the differences are in millibars.

Station	DIFF	σ	Station	DIFF	σ
01	0.274	0.216	26	0.146	0.769
02	0.566	0.336	27	0.712	0.376
03	-1.195	0.293	28	-1.509	0.788
04	-0.055	0.349	29	-1.363	0.533
05	1.075	0.413	30	-0.069	0.443
06	0.569	0.681	31	-0.040	0.468
07	1.361	0.473	32	2.505	0.600
08	0.712	0.335	33	0.146	0.267
09	-0.880	0.422	34	-0.220	0.249
10	-1.833	0.727	35	2.461	0.528
11	-0.120	0.470	36	0.267	0.386
12	0.261	0.566	37	0.072	0.335
13	0.718	0.353	38	-0.072	0.436
14	-0.091	0.259	39	-0.513	0.325
15	-0.318	0.344	40	-0.145	0.285
16	-0.577	0.276	41	1.899	0.356
17	0.335	0.349	42	0.162	0.222
18	0.171	0.319	43	-0.618	0.508
19	-1.025	0.197	44	0.156	0.597
20	1.171	0.461	45	-0.804	0.449
21	2.088	0.437	46	0.070	0.432
22	1.568	0.216	47	0.035	0.234
23	-0.087	0.349	48	-0.040	0.295
24	1.538	0.965	49	-0.739	0.330
25	0.952	0.360	50	-0.268	0.486

Therefore, it would appear that the Barnes objective analysis scheme is producing valid results.

Table 3.4 shows a comparison between the ten station buddy check results and the average differences obtained with the Barnes analysis for the same ten stations. All but two of the stations have the same sign. An explanation for the change in sign for PAM #26 is that the

Table 3.3 This table shows the corrections obtained from the Barnes analysis scheme for the five consecutive hours beginning with 1000 UTC on 14 February 1986. Units for the corrections are millibars.

Station	1000	1100	1200	1300	1400	Station	1000	1100	1200	1300	1400
01	-0.11	-0.21	0.16	0.01	0.14	26	-0.29	-0.16	-0.35	-0.11	0.09
02	0.39	0.53	0.91	0.21	0.66	27	1.08	0.95	1.32	1.75	1.58
03	-1.23	-1.08	-0.95	-1.29	-0.94	28	-1.99	-2.18	-1.63	-1.72	-1.90
04	-0.39	0.15	-0.17	-0.23	-0.20	29	-2.13	-2.08	-1.56	-1.35	-1.59
05	1.20	0.90	0.73	0.60	0.41	30	-0.37	-0.15	-0.58	0.31	0.24
06	0.45	0.05	0.63	0.25	0.53	31	0.46	0.03	0.66	-0.43	0
07	0.92	1.29	1.85	0.89	1.25	32	2.11	1.28	2.01	1.95	1.83
08	0.49	0.63	1.01	0.62	0.65	33	0.20	-0.18	0.32	0.10	0.14
09	-1.22	-1.07	-1.24	-1.43	-1.36	34	-0.79	-0.42	-0.51	-0.34	-0.30
10	-1.42	-1.36	-1.52	-1.72	-1.29	35	1.79	1.97	1.56	2.41	2.29
11	-0.26	-0.95	-0.26	-0.47	-0.87	36	-0.06	0.03	-0.30	0.36	0.27
12	-0.24	0.45	0.52	0.39	0.28	37	-0.20	-0.23	-0.79	0.03	-0.28
13	0.58	1.04	1.17	0.83	0.80	38	-0.38	-0.92	0.21	0.11	-0.06
14	0.33	0.06	0.06	-0.01	0.19	39	1.02	0.96	-0.29	-1.04	-1.34
15	-0.37	-0.44	-0.29	-0.33	-0.07	40	-0.71	-0.78	-0.22	-0.85	-0.25
16	-0.47	-1.09	-0.25	-0.46	-0.79	41	1.43	1.68	1.44	1.84	1.73
17	-0.16	0.13	0.10	0.02	-0.12	42	-0.44	-0.43	-0.17	-0.07	-0.31
18	-0.65	0.35	0.09	0.20	-0.42	43	-0.55	-0.75	-0.67	-1.00	-1.10
19	-1.05	-0.64	-1.23	-1.49	-1.30	44	-0.64	0.20	0.33	-0.09	0.01
20	0.94	0.99	1.15	1.43	1.17	45	-1.34	-1.98	-1.44	-1.74	-0.59
21	2.22	2.02	2.30	2.15	1.97	46	-0.34	-0.55	-0.33	-0.51	0.37
22	0.84	0.02	1.23	0.78	1.09	47	0.21	-0.47	-0.10	0.33	0.78
23	-0.27	-0.13	-0.49	-0.24	-0.27	48	-0.05	-0.17	-0.11	-0.07	0.31
24	*****	*****	1.59	1.64	2.00	49	-0.95	-0.48	-0.73	-0.91	-0.41
25	0.45	0.39	0.29	0.26	1.06	50	-0.34	-0.16	-0.30	-0.21	-0.68

station is closer to Winston-Salem (INT) than Greensboro (GSO) so the Barnes analysis would weigh more heavily the Winston-Salem altimeter setting than that of Greensboro. Also, one would expect the average differences of the Barnes analysis and the buddy check to differ because the former method incorporates data from surrounding stations into the interpolated altimeter setting instead of data from only one station. Thus, at least the synoptic and meso-α scale pressure field

Table 3.4 Comparison between the differences obtained from the Buddy Check and Barnes Analysis methods. Units of the "corrections" are in millibars.

Station	Buddy Check	Barnes Analysis
01	0.211	0.274
03	-0.682	-1.195
06	0.693	0.569
09	-1.475	-0.880
15	1.501	-0.318
21	2.522	2.088
26	-0.293	0.148
33	1.730	0.146
34	0.741	-0.220
45	0.777	-0.804
ΣX	5.725	-0.192
Mean	0.573	-0.019
σ	1.128	0.883

are accounted for.

One might expect the Barnes method which accounts for the synoptic-scale pressure patterns to represent an improvement over the buddy check method. In order to determine whether there is a statistically significant difference between the two methods, a test of the variances of each method was conducted. A Chi-squared test was performed using the following information:

σ_{BC} = 1.128 mb (standard deviation for buddy check method)

σ_{BA} = 0.883 mb (standard deviation for Barnes method)

Level of significance, α = 0.05

The null hypothesis and the alternate hypothesis were taken as

$$H_0: \quad \sigma^2_{BA} = \sigma^2_{BC} \text{ and}$$

$$H_1: \quad \sigma^2_{BA} < \sigma^2_{BC}$$

From Table VI in Walpole and Meyers (1978), and using v = 9 degrees of freedom, the critical region was taken as $X^2 < 3.325$, where $X^2 = (n-1)\sigma^2_{BA}/\sigma^2_{BC}$ In this test if a calculated X^2 is less than 3.325, the null hypothesis can be rejected and the alternate hypothesis accepted. The value of X^2 was found to be 5.515. Since this is greater than the critical value of 3.325, the null hypothesis can be accepted and it can be concluded that there is no significant difference, statistically, between the two methods. However, the Barnes analysis method will be used for the pressure corrections because not all of the PAM II stations have a nearby NWS station with which to conduct a buddy check.

As can be seen from Table 3.2, some of the differences have absolute values greater than 1 mb. In order to determine if these large differences are the result of PAM II elevation error or just instrument offsets, a check of the NCAR field calibration data was performed. The field calibration differences were averaged for each station and these averages were compared to the stations whose average Barnes differences exceed +/- 1 mb. This comparison is presented in Table 3.5. In most cases where the magnitude of the Barnes scheme correction exceeds 1 mb, the average field-calibration difference also exceeds 1 mb. However, some stations experience a sign change between the field calibrations and the Barnes analysis. As a result, this check would appear to be inconclusive on whether the large corrections

Table 3.5 Comparison between the field calibration data and the Barnes Analysis data for selected PAM II sites. Units are millibars.

Station	Calibration	Barnes
03	1.255	-1.195
05	1.470	1.075
07	2.140	1.361
10	1.640	-1.833
19	0.717	-1.025
20	1.667	1.171
21	2.473	2.088
22	2.313	1.568
24	2.506	1.538
28	0.498	-1.509
29	0.573	-1.363
32	2.225	2.505
35	2.793	2.461
41	2.190	1.899

are due to elevation errors.

A second check into this matter of large corrections was conducted by examining the local relief of those stations listed in Table 3.5. The effect of local relief hinges on the uncertainty of the exact station location and exact terrain elevation. Once the station locations were found on a topographic map, a half-kilometer diameter circle was drawn, centered on the station. The resolution of the topographic maps used would allow the station location to be pinpointed to within a half-kilometer. The maximum and minimum elevations within this circle were recorded and the elevation differences were found and are displayed in Table 3.6.

From Table 3.6, only stations 5, 19, 20, 28, and 29 have elevation

Table 3.6. Shows the elevation differences (in meters) within a half-kilometer circle centered at the station.

Station	Difference
03	6
05	13
19	10
20	10
21	3
22	3
24	6
28	20
29	25
32	3
35	3
41	3

differences large enough to account for corrections exceeding 1 mb. These five stations are located in the western Piedmont and the Appalachian regions of North Carolina, South Carolina, and Virginia. Those stations located in the Coastal Plain only had elevation differences of 3-6 m, which would not account for their large corrections. From this it would appear that only the corrections for the stations in the higher elevations may be the result of errors in station elevation. In light of the mixed results, it seems easier to apply the large corrections to the station pressure rather than to correct the elevations of an uncertain number of PAM II stations.

After applying the correction to the observed altimeter setting, a new station pressure was calculated using the following equation:

$$P = [\ (ALSTG)^n - (P_0^n aH/T_0)\ ]^{1/n} + 0.3. \quad (3.4)$$

The observed station pressure was subtracted from this "corrected" station pressure to find the pressure correction value. Table 3.7 gives the station pressure correction for each PAM II station.

3.2 Reduction of Station Pressures to Sea Level

The procedure for reducing the corrected station pressures to sea level was taken directly from the Manual of Barometry (1963). The procedure, as outlined in the Manual of Barometry, is based upon the hypsometric equation:

$$P_0 = P \cdot 10^{(KH/T_{MV})}, \quad (3.5)$$

where P_0 = sea level pressure (mb)

P = station pressure (mb)

K = hypsometric constant (0.0266895°R/m)

H = station elevation (m)

T_{MV} = mean virtual temperature (°R)

Use of the hypsometric equation assumes a vertical air column in which the effects of vertical acceleration are negligible. This assumption describes a hydrostatic condition in which the weight of each layer in the air column is in balance with the pressure difference between the lower and upper level surfaces confining the layer. The Manual of Barometry provides tables of values of the ratio $P_0/P = r$ which are based on the elevation and mean virtual temperature

Table 3.7 Pressure corrections in millibars to be applied to the station pressure recorded at the PAM II stations.

Station	Correction	Station	Correction
01	-0.27	26	-0.15
02	-0.57	27	-0.70
03	+1.18	28	+1.40
04	+0.05	29	+1.26
05	-1.07	30	+0.07
06	-0.57	31	+0.04
07	-1.36	32	-2.50
08	-0.71	33	-0.15
09	+0.86	34	+0.21
10	+1.80	35	-2.46
11	+0.12	36	-0.27
12	-0.26	37	-0.08
13	-0.71	38	+0.06
14	+0.08	39	+0.50
15	+0.31	40	+0.15
16	+0.58	41	-1.90
17	-0.34	42	-0.16
18	-0.17	43	+0.62
19	+1.01	44	-0.15
20	-1.16	45	+0.81
21	-2.09	46	-0.07
22	-1.57	47	-0.04
23	+0.09	48	+0.04
24	-1.57	49	+0.74
25	-0.94	50	+0.26

of the station. In this research, r was calculated using the equation:

$$r = 10^{(\text{illegible})}. \qquad (3.6)$$

Virtual temperature is used in this procedure in order to account for the effect of water vapor on the density of moist air. According to the Manual of Barometry, the mean virtual temperature can be found from the following equation:

$$T_{MV} = T_0 + t_s + aH/2 + e_s C_h + F. \qquad (3.7)$$

where T_0 is the conversion of temperature into absolute units, either 273 K or 459.7°R and t_s is the station temperature argument, which is simply the average of the observed temperature and the temperature recorded twelve hours earlier:

$$t_s = (t_0 + t_{-12})/2. \qquad (3.8)$$

The standard lapse rate correction is aH/2, where a is the standard lapse rate; either 0.0065°C/m or 0.117°F/m. Using this correction means that the mean temperature of the air column is considered greater than the temperature argument at the station (t_s) by aH/2. This is the same as saying the mean temperature is the linear average of t_s and the temperature at sea level, based on the assumption that the lapse rate has a standard value.

The humidity correction is $e_s C_h$ with e_s being the saturated vapor pressure (in mb) at the station at the time of the observation and C_h being a known function of station elevation in °F/mb. This humidity correction is necessary because the density of moist air is less than the density of dry air provided that the pressure and temperature are the same. The quantity $e_s C_h$ is intended to represent a correction considered as a difference between the mean virtual temperature of the fictitious air column and the mean dry-bulb temperature of the fictitious air column. The quantity e_s refers to the surface, but the quantity $e_s C_h$ refers to the entire air column.

The correction for the plateau effect and local lapse rate anomaly

is F. The plateau effect correction is introduced so the amplitude of the annual variation of pressure reduced to sea level is approximately the same at all stations regardless of elevation. The local lapse rate anomaly correction takes into account any deviation of the assumed local lapse rate from the standard lapse rate. For stations with elevations of 305 m or lower, F is determined on the basis of the annual mean station temperature. For stations exceeding 305 m in elevation, F is determined by geographic location, elevation, and climatological conditions.

In calculating the sea level pressure for each PAM II station, estimates of the annual mean temperature and saturated vapor pressure had to be made. An annual mean temperature for each station was obtained by using the annual mean temperatures of the nearby NWS stations.

The saturated vapor pressure was obtained from Table 7.2.1 in the Manual of Barometry. The method used in obtaining an e_s for stations not listed in the table is to select the data from the station in the table that has similar topographic and climatological conditions as the station in question. Figure 3.6 shows the PAM II stations and the NWS station from which saturated vapor pressure values were obtained for the PAM II stations. The hatched regions indicate the PAM II stations for which data was obtained by averaging data from two NWS stations.

To illustrate the somewhat involved process of pressure reduction described above, suppose we wish to obtain sea-level pressures for 1200 UTC 25 February 1986. First, the temperature argument for each PAM II

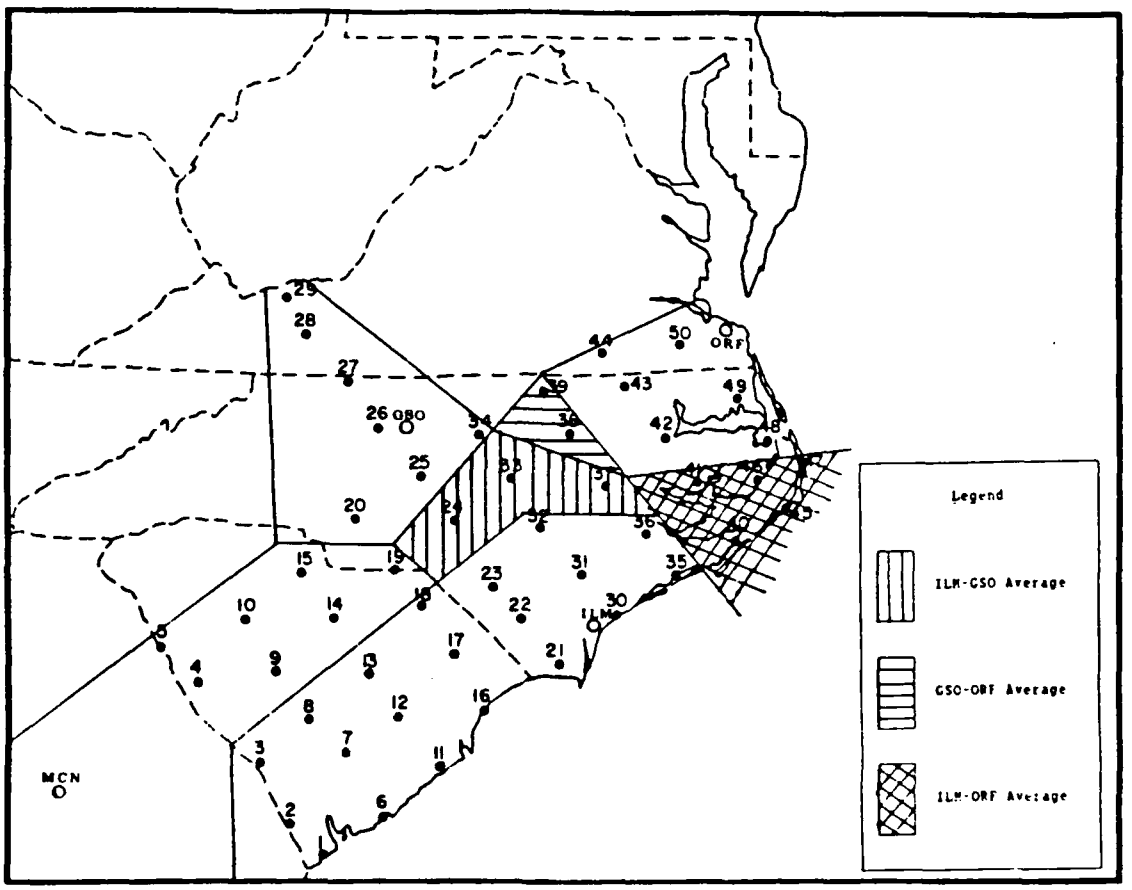

Figure 3.6. Map showing the NWS station(s) used in determining vapor pressure data for the PAM II stations for use in the Sea-Level Pressure Reduction Procedure outlined in the Manual of Barometry (1961). The unhatched areas indicate that the data for the PAM II stations were obtained from the lone NWS station in the area.

station is calculated using the temperatures recorded at 1200 UTC and 0000 UTC. Based on the temperature argument for each station, a saturated vapor pressure is found from Table 7.2.1 in the Manual of Barometry. Next, the standard lapse rate and humidity corrections are found from Table 7.3 in the Manual of Barometry and F is found using Table 7.4.1 in the Manual of Barometry. Next, the mean virtual

temperature is calculated from equation (3.7).

Once the mean virtual temperature is found, r can be calculated from equation (3.6) with K = 0.0266895°R/m. Sea level pressure is then found by multiplying the corrected station pressure by r.

The resulting sea-level pressures for the PAM II stations for our example are plotted along with the NWS sea-level pressures and the resulting analysis is shown in Figure 3.7a. This analyzed pressure field matches well with the National Meteorological Center (NMC) analysis of the same time (Figure 3.7b). Since the analyses in Figure 3.7 agree then it follows that the PAM II pressures agree well with the NWS pressure field.

This method of reduction to sea level is rather complicated as one must consult tables to obtain the parameters C_h and F in (3.7). In an effort to obtain a more simplified method, an attempt was made to determine the magnitude of the virtual temperature deviation permissible in order to maintain a sea-level pressure within 0.3 mb. Figure 3.8 shows the change in virtual temperature required to obtain a sea-level pressure deviation of 0.3 mb for station elevations up to 800 m. From Figure 3.8 it can be seen that the virtual temperature deviation decreases with height to around 1.5 °F at 800 m. The value of F in Equation (3.7) is usually around 10°F so based on Figure 3.8, F must be retained. The value of the term $(aH/2 + e_s C_h)$ is between 1.5°F and 2.5°F. This term begins to become significant for stations with elevations near 500 m. The entire term can be approximated by a value of 2°F because, even at the term's extremes, the virtual temperature

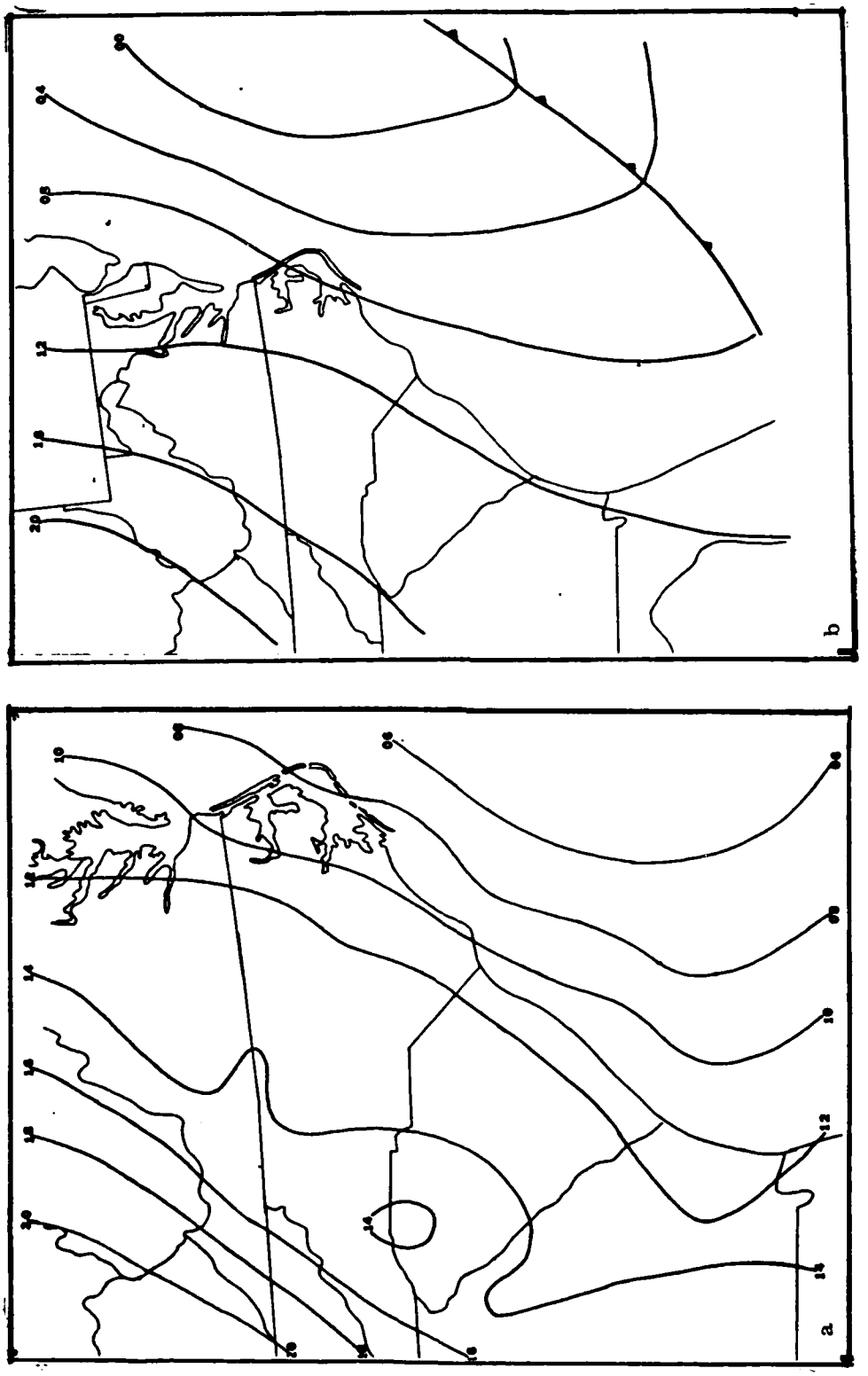

Figure 3.7. (a) NWS - FNM 11 sea-level pressure analysis for 1200 UTC 25 February 1986. (b) NMC sea-level pressure analysis for the same time.

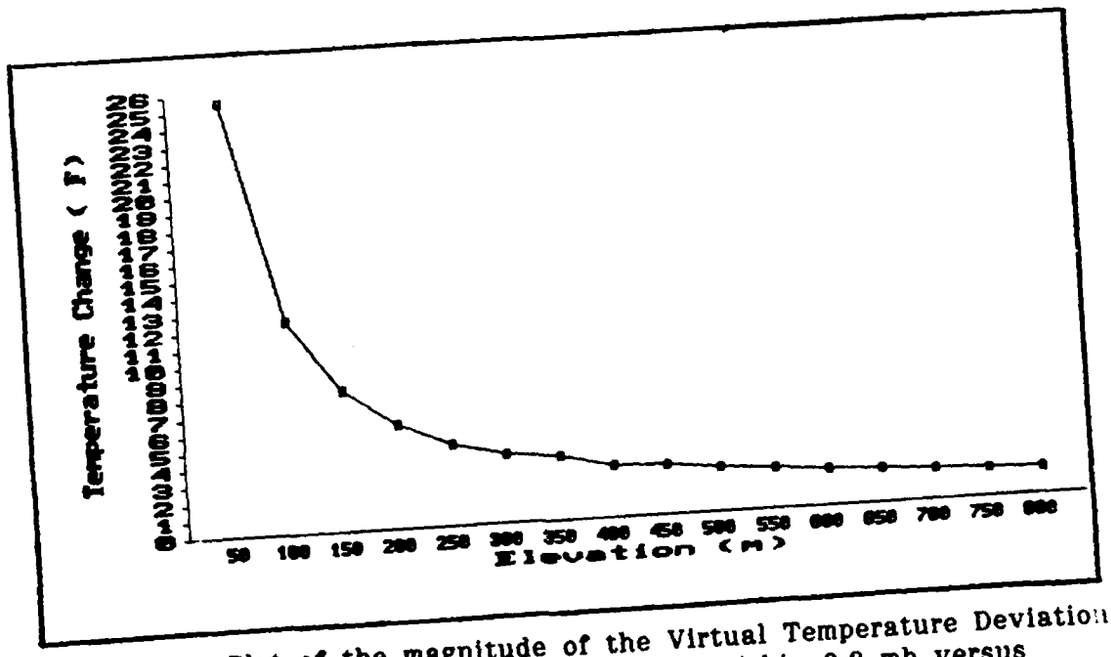

Figure 3.8. Plot of the magnitude of the Virtual Temperature Deviation permissible to maintain a sea-level pressure within 0.3 mb versus Station Elevation.

will only be off by 0.5°F, an error which does not create a significant change in the sea-level pressure. Thus, equation (3.7) reduces to:

$$T_{mv} = T_0 + t_s + F + 2°F. \qquad (3.9)$$

Equation (3.9) still contains F which requires the use of Table 7.4.1 in the Manual of Barometry (1963). Using Table 7.4.1 (reproduced in Figure 3.9) an empirical formula was derived to solve for F as follows:

An average $F(t_s)$ per °F for a t_s of 0°F was calculated and found to be 0.4375. An average $F(t_s)$ per °F for each annual mean temperature (t_m) over a t_s range of 0°F to 70°F was calculated and found to be 0.434. An empirical formula for F was developed using the $F(t_s)$ for a

t_s of 0°F and a t_{sn} of 35°F from Table 7.4.1 as the base value. The empirical formula is

$$F = 14.3°F + 0.4375(t_{sn} - 35°F) - 0.434t_s. \qquad (3.10)$$

Calculating a sea level pressure from equations (3.9) and (3.10) and comparing the results illustrated in Figure 3.7 reveals that these new sea level pressures are within 0.3 mb for those stations with elevations of 305 m or less. Therefore, it can be concluded that, to a first approximation, this revised method can be used to reduce the PAM II station pressures to sea level. Table 3.8 illustrates the comparison of the two methods for 1200 UTC 25 February 1986.

TABLE 7.4.1

Correction for Plateau Effect and Local Lapse Rate Anomaly, $F(t_s)$, for Continental U.S. Stations Having Elevations of ≤05 gpm (1,000 Feet) or Lower

[$F(t_s)$ Data Are Tabulated as a Function of Station Temperature Argument, t_s.]

Annual normal station temperature (t_{sn}) °F.	Station temperature argument, t_s, in ° F.									
	−70°	−60°	−50°	−40°	−30°	−20°	−10°	0°	+10°	+20°
	° F.	° F.	° F.	° F.	° F.	° F.	° F.	° F.	° F.	° F.
35.0	32.3	30.6	28.6	26.3	23.7	20.9	17.7	14.3	10.6	6.6
40.0	34.0	32.3	30.4	28.2	25.7	22.9	19.8	16.4	12.8	8.8
45.0	....	34.1	32.2	30.1	27.6	24.9	21.9	18.6	15.0	11.1
50.0	....	35.9	34.1	32.0	29.6	26.9	24.0	20.7	17.2	13.4
55.0	....	....	35.9	33.9	31.6	29.0	26.1	22.9	19.4	15.7
60.0	....	....	....	35.8	33.6	31.0	28.2	25.1	21.7	18.0
65.0	....	....	....	....	35.6	33.1	30.4	27.3	23.9	20.3
70.0	....	....	....	....	37.7	35.2	32.6	29.6	26.3	22.7
75.0	....	....	....	....	39.7	37.4	34.8	31.8	28.6	25.0

Annual normal station temperature (t_{sn}) °F.	Station temperature argument, t_s, in ° F.									
	+30°	+40°	+50°	+60°	+70°	+80°	+90°	+100°	+110°	+120°
	° F.	° F.	° F.	° F.	° F.	° F.	° F.	° F.	° F.	° F.
35.0	2.3	−2.3	−7.3	−12.5	−18.1	−23.9	−29.9	−36.2	−42.8	....
40.0	4.5	0.0	−4.9	−10.1	−15.6	−21.3	−27.4	−33.7	−40.1	....
45.0	6.9	2.4	−2.4	− 7.6	−13.0	−18.8	−24.8	−31.1	−37.5	....
50.0	9.2	4.7	0.0	− 5.1	−10.5	−16.2	−22.2	−28.4	−34.8	....
55.0	11.6	7.2	2.5	− 2.5	− 7.9	−13.6	−19.5	−25.7	−32.0	....
60.0	13.9	9.6	5.0	0.0	− 5.3	−10.9	−16.9	−23.0	−29.3	−35.9
65.0	16.4	12.1	7.5	2.6	− 2.7	− 8.2	−14.1	−20.3	−26.5	−33.0
70.0	18.8	14.6	10.0	5.1	0.0	− 5.5	−11.4	−17.5	−23.6	−30.2
75.0	21.3	17.1	12.6	7.8	2.7	− 2.8	− 8.6	−14.7	−20.8	−27.3

Figure 3.9. Table 7.4.1 from the Manual of Barometry.

Table 3.8 Comparison between using the Manual of Barometry (MoB) method and the revised method of reducing PAM II station pressures to sea level for 1200 UTC 25 February 1986. Units of the sea level pressures are millibars.

Station	MoB	Revised	Station	MoB	Revised
01	1011.51	1011.52	26	1012.99	1013.28
02	1012.02	1012.13	27	1013.73	1014.11
03	1013.19	1013.24	28	1015.16	1015.75
04	1014.13	1014.22	29	1017.44	1017.03
05	1014.51	1014.64	30	1010.07	1010.07
06	1011.52	1011.52	31	1011.12	1011.13
07	1012.91	1012.94	32	1012.08	1012.13
08	1013.23	1013.32	33	1013.30	1013.40
09	1013.75	1014.34	34	1013.66	1013.81
10	1014.83	1014.95	35	1009.32	1009.32
11	1011.72	1011.72	36	1010.14	1010.14
12	1012.78	1012.79	37	1011.94	1011.97
13	1012.92	1012.95	38	1013.07	1013.14
14	1013.54	1013.64	39	1013.08	1013.20
15	1014.66	1014.64	40	1008.76	1008.75
16	1010.66	1010.68	41	1009.91	1009.91
17	1012.46	1012.47	42	1011.23	1011.24
18	1013.18	1013.20	43	1012.39	1012.41
19	1013.44	1013.54	44	1013.45	1013.52
20	1013.76	1013.89	45	1007.87	1007.87
21	1010.23	1010.22	46	1008.42	1008.42
22	1011.50	1011.52	47	1007.58	1007.57
23	1012.55	1012.59	48	1008.71	1008.71
24	1013.11	1013.24	49	1009.65	1009.66
25	1014.02	1014.21	50	1011.81	1011.83

4. ALTERNATE METHOD FOR PRESSURE REDUCTION

The NWS reduction procedure is rather involved and includes a number of assumptions to arrive at the sea-level pressure. In this section, another method of pressure reduction, introduced by Pielke and Cram (1987), is explored to eliminate the arbitrariness of the standard reduction procedure. The method first calculates a geostrophic wind field and then calculates the surface pressure corresponding to this wind field.

In this research, both the standard pressure-reduction method and the Pielke and Cram method will be applied to a cold-air damming situation on 25 January 1986 (GALE IOP 2). The 1200 UTC data are being used because in the routine National Meteorological Center (NMC) analysis, the observed surface winds are nearly perpendicular to the isobars over North and South Carolina. The pressure and geostrophic wind fields computed from each method will be compared in order to determine the effect of the assumptions in the standard reduction procedure. The geostrophic wind fields calculated from each method will be compared to the observed surface wind field in an attempt to determine the true ageostrophic wind components during a cold-air damming situation.

4.1 Theory

The method introduced by Pielke and Cram (1987) uses a terrain-following coordinate system to obtain the horizontal pressure field from observations obtained on a sloping surface. The vertical coordinate of this system was developed by Pielke and Martin (1981) and

is defined as:

$$\sigma = s \frac{z - z_G}{s - z_G}, \qquad (4.1)$$

where σ is the generalized vertical coordinate, s is an arbitrary height in the atmosphere (usually taken as the top of the model), z_G is the terrain elevation, and z is the height above the surface (Pielke and Martin, 1981). Figure 4.1 illustrates an example of the terrain following coordinate system (Pielke, 1984).

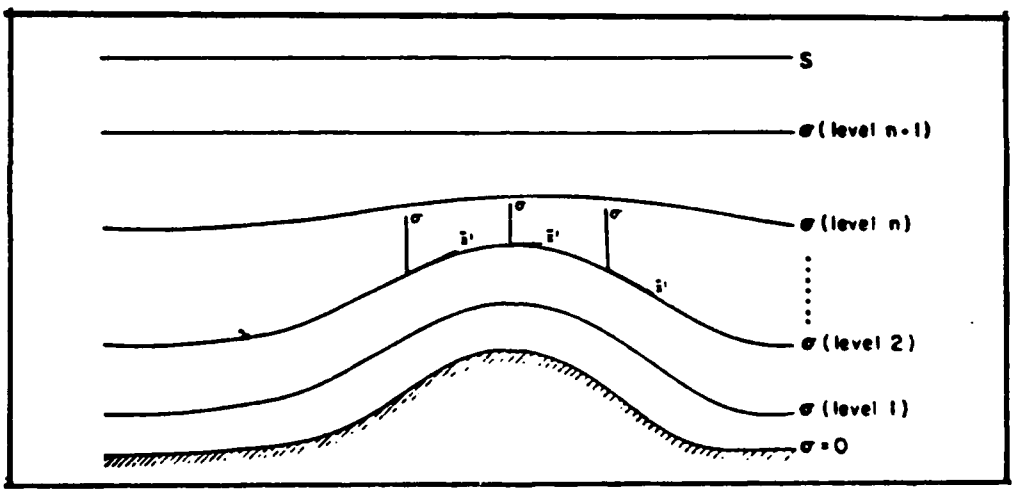

Figure 4.1. Schematic of the terrain-following coordinate system, σ (from Pielke, 1984).

Pielke (1984) shows that the simplified momentum equation for terrain-following flow can be written as:

$$\frac{du}{dt} = -\theta \frac{\partial \pi}{\partial x} + g \frac{\sigma - s}{s} \frac{\partial z_G}{\partial x} + fv$$
$$\frac{dv}{dt} = -\theta \frac{\partial \pi}{\partial y} + g \frac{\sigma - s}{s} \frac{\partial z_G}{\partial y} - fu \qquad (4.2)$$

where u and v are the σ-parallel flow in the east-west (x) and north-south (y) directions, respectively, f is the Coriolis parameter, Θ is the potential temperature, g is the acceleration due to gravity, $\pi = c_p T/\Theta = c_p(p/p_0)^{R/cp}$, and T is the temperature. The scaled pressure, π, is directly related to pressure, p. The pressure-gradient term is now written as the sum of the π-gradient along a sigma surface and the terrain-gradient term (Pielke et al., 1985).

Neglecting acceleration, the momentum equation (4.2) reduces to the geostrophic wind equation in the σ-coordinate system:

$$v_g = \frac{\theta}{f}\frac{\partial \pi}{\partial x} - \frac{g}{f}\frac{\sigma - s}{s}\frac{\partial z_G}{\partial x},$$
$$u_g = -\frac{\theta}{f}\frac{\partial \pi}{\partial y} + \frac{g}{f}\frac{\sigma - s}{s}\frac{\partial z_G}{\partial y}. \qquad (4.3)$$

On a horizontal, level surface (no terrain slope) Equation (4.3) reduces to the geostrophic wind in the x-y-z coordinate system:

$$v_g = \frac{\theta}{f}\frac{\partial \pi}{\partial x},$$
$$u_g = -\frac{\theta}{f}\frac{\partial \pi}{\partial y}. \qquad (4.4)$$

At the surface, $z = z_G$, so from (4.1) $\sigma = 0$ and (4.3) becomes:

$$v_g = \frac{\theta}{f}\frac{\partial \pi}{\partial x} + \frac{g}{f}\frac{\partial z_G}{\partial x},$$
$$u_g = -\frac{\theta}{f}\frac{\partial \pi}{\partial y} - \frac{g}{f}\frac{\partial z_G}{\partial y}. \qquad (4.5)$$

This equation for the surface geostrophic wind is then used to obtain the horizontal pressure gradient over flat terrain:

$$v_g = \frac{\theta}{f}\frac{\partial \pi}{\partial x} + \frac{g}{f}\frac{\partial z_G}{\partial x} = \frac{\theta}{f}\frac{\partial \tilde{\pi}}{\partial x} \,,$$
$$u_g = -\frac{\theta}{f}\frac{\partial \pi}{\partial y} - \frac{g}{f}\frac{\partial z_G}{\partial y} = -\frac{\theta}{f}\frac{\partial \tilde{\pi}}{\partial y} \,. \qquad (4.6)$$

The pressure on a flat terrain surface, $\tilde{\pi}$, can be obtained from the equation:

$$\frac{\partial^2 \tilde{\pi}}{\partial x^2} + \frac{\partial^2 \tilde{\pi}}{\partial y^2} = \frac{\partial}{\partial x}\left(\frac{v_g f}{\theta}\right) - \frac{\partial}{\partial y}\left(\frac{u_g f}{\theta}\right) \,. \qquad (4.7)$$

Here, u_g and v_g are obtained from (4.5).

The component of the σ-system pressure gradient of interest is the one on a flat surface. Since in a flat, mean sea-level, z-system the geostrophic wind is non-divergent except for the variation of f, v_g is differentiated with respect to x and u_g is differentiated with respect to y and subtracted to yield an elliptic equation for $\tilde{\pi}$ (Pielke and Cram, 1987). Note that equation (4.7) is the geostrophic relative vorticity equation in this coordinate system.

4.2 PROCEDURE

The data involved in this procedure are obtained from the stations in Figure 3.4 and the fifty PAM II stations. First, the potential temperature, θ. and the modified pressure argument, π, are computed from the temperature and station pressure. Then, a gridded array of

height, Θ, and π is obtained from the Barnes objective analysis with a weight parameter, k, of 10000 km^2 and a convergence parameter, Γ, of 0.3 (same as discussed in Chapter 3).

The three gridded arrays are used in obtaining the u and v components of the geostrophic wind for each grid point from equation (4.5). From the u and v components, a geostrophic wind field is generated and is shown in Figure 4.2.

The final step is obtaining the pressure field that would produce the geostrophic wind components calculated in the previous step. To obtain the pressure field, equation (4.7) is solved using a relaxation method. The right side of equation (4.7) is called the forcing function. A first guess of the $\tilde{\pi}$ field is provided and the computer corrects this guess until the resulting $\tilde{\pi}$ field is within a certain tolerance of the forcing function (i. e. the $\tilde{\pi}$ field is relaxed).

For this research, the tolerance used is 0.01 $^{\circ}K^{-1}s^{-1}$ and the relaxation factor is 0.30; however, later experiments indicate a relaxation factor around 0.40 is more efficient. For the boundary conditions, Pielke and Cram (1987) employed pressures reduced to sea level using a standard lapse rate. As a result, this research employs altimeter settings for the boundary conditions and a Barnes analyzed field of altimeter settings for the first guess.

The altimeter settings are converted to $\tilde{\pi}$ using the equation:

$$\tilde{\pi} = c_p \, (p/1000)^{K} \, , \qquad (4.8)$$

with $K = R/c_p$ and p replaced with the altimeter setting. Once the $\tilde{\pi}$

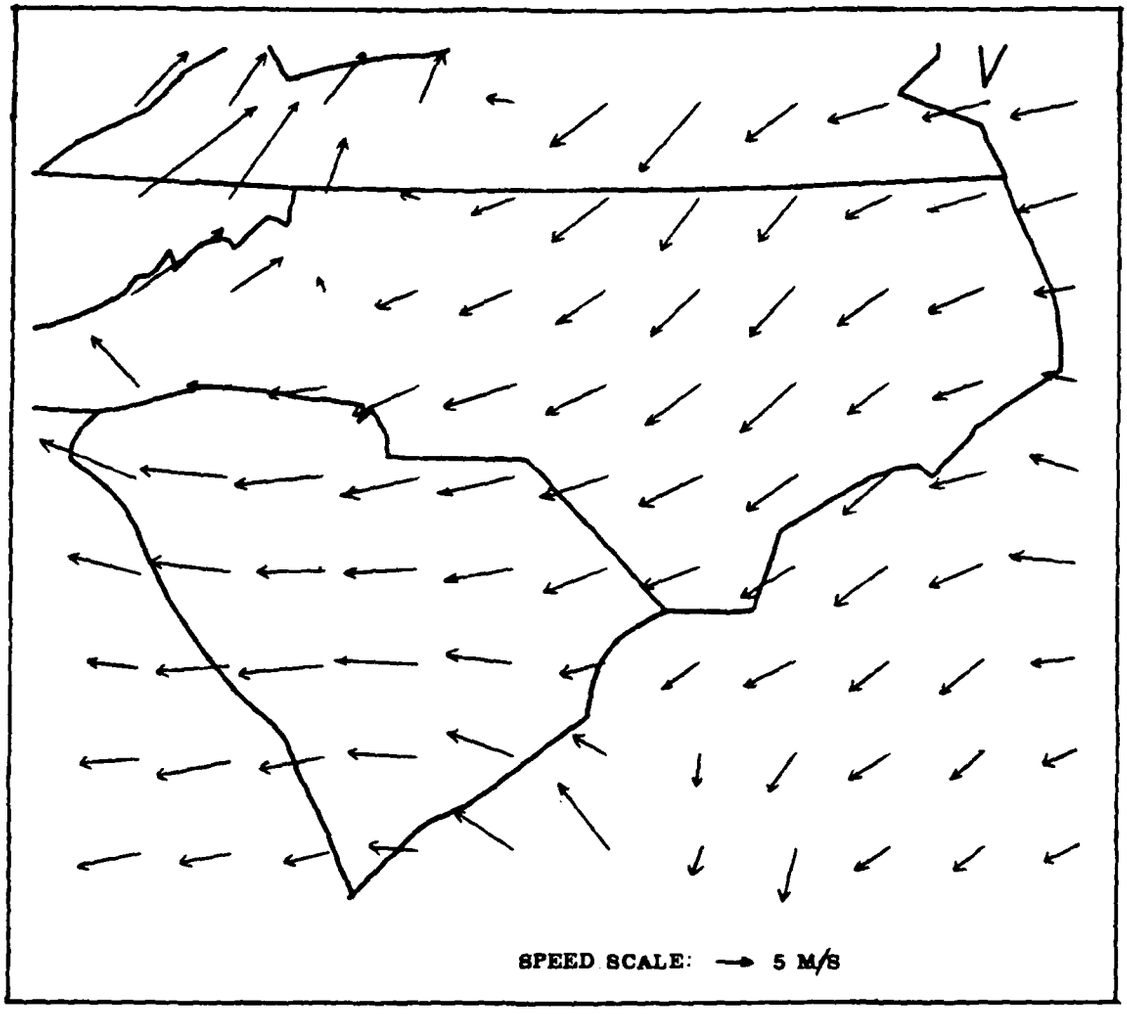

Figure 4.2. Geostrophic wind field computed from equation (4.5).

field is relaxed, the individual $\tilde{\pi}$s are converted to pressure by:

$$p = 1000(\tilde{\pi}/c_p)^{1/\kappa} . \qquad (4.9)$$

The resulting analyzed pressure field is shown as Figure 4.3.

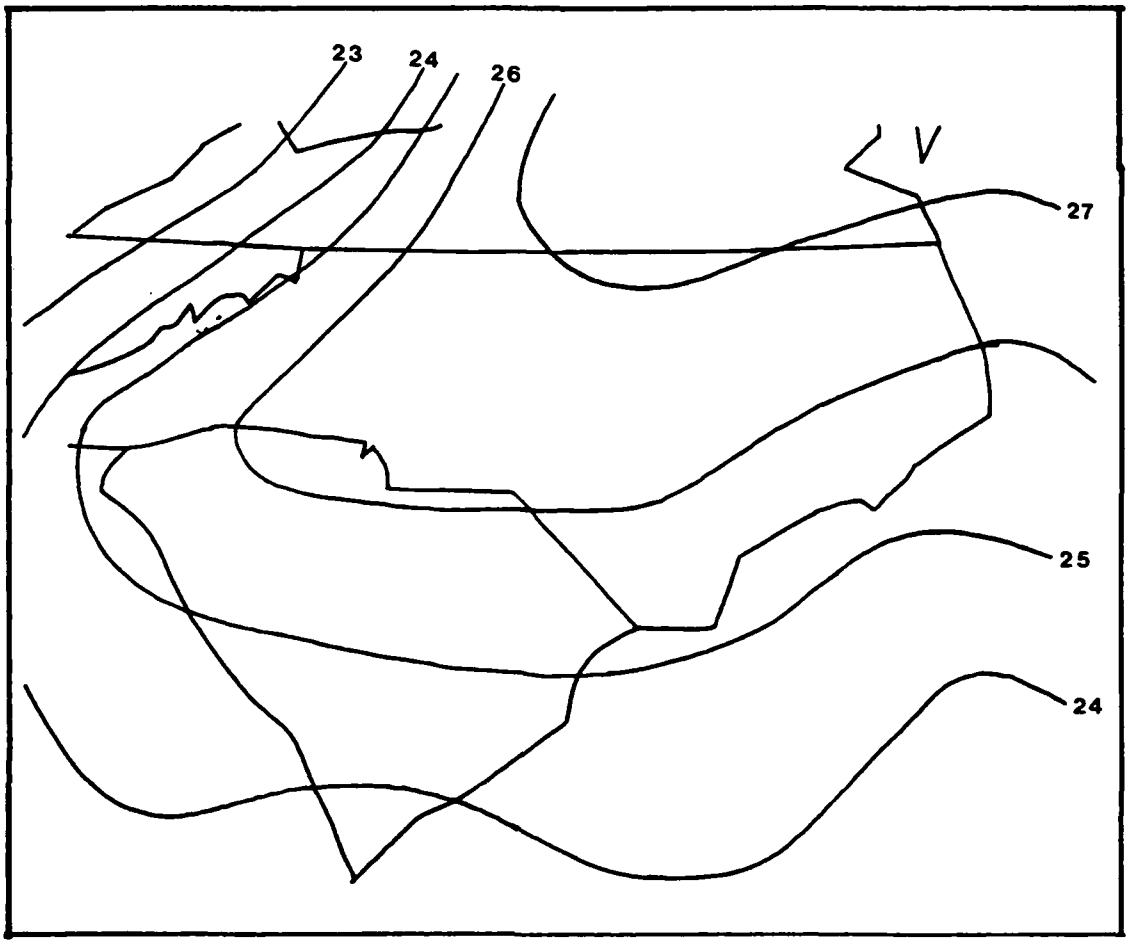

Figure 4.3. Horizontal pressure field corresponding to the geostrophic wind field shown in Figure 4.2.

4.3 RESULTS

The surface pressure analysis of Figure 4.3 has the same general pattern as the sea-level pressure analysis shown in Figure 4.4. A high pressure ridge extends through the Carolinas with an inverted trough along the coast. However, the ridge over western North and South Carolina appears to be shifted to the west in Figure 4.3. The standard pressure reduction procedure resulted in the sea-level pressures being

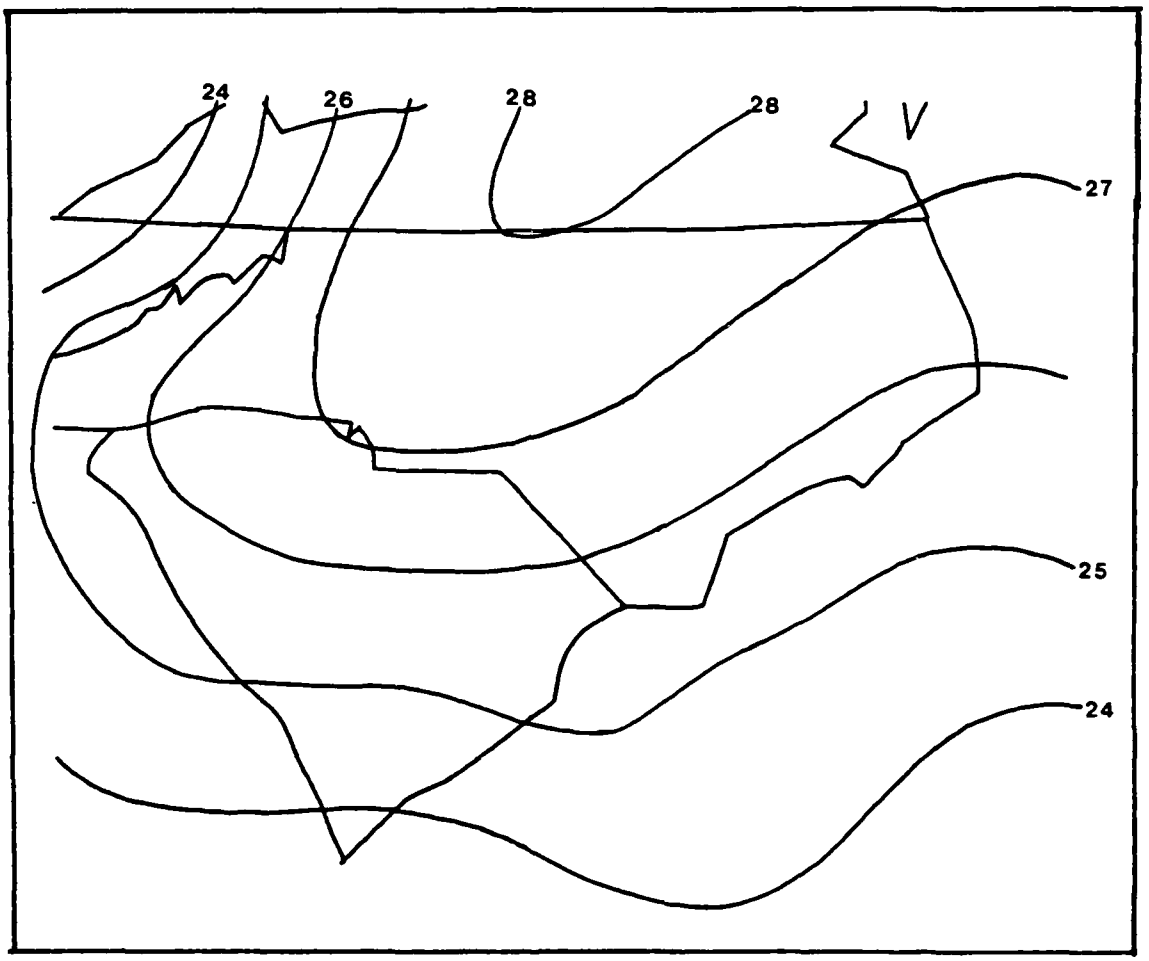

Figure 4.4. Sea-level pressure analysis for 1200 UTC 25 January 1986.

about 1 mb higher than the surface pressure field calculated in the previous section. The pressure gradient over the mountains appears to be greater in Figure 4.3 than in Figure 4.4. In a cold-air damming situation, one would expect a tight packing of the isobars at the mountains due to the cold air being dammed against the mountains. It would seem that the assumptions in the standard reduction procedure reduce this damming effect on the pressure field and result in a slight underestimate of the gradient.

One other item to note about the comparison of Figures 4.3 and 4.4 is the isobars over the coastal waters do not match as would be expected. In both procedures, the pressure data recorded at the marine stations did not need to be reduced, but the altimeter equation subtracts 0.3 mb from the station pressure. This subtraction accounts for the difference in the isobars over the water.

Moving on to the comparison between the surface geostrophic wind field depicted in Figure 4.2 and the geostrophic wind field calculated from the sea-level pressures depicted in Figure 4.5, the same general pattern is found; however, the ridge in the wind field is shifted westward in Figure 4.2. The cause of this shift could be the result of the dominance of the terrain term in equation (4.5). In the absence of a pressure gradient, the effect of the terrain is to produce a ridge over the mountains and, on a flat terrain, the effect of the pressure term is to produce a trough over the mountains. These two effects should almost cancel each other in equation (4.5), but because high pressure is dominating the region, the contribution of the pressure term is reduced allowing the westward shift of the ridge in the wind field in Figure 4.2.

Overlaying Figure 4.2 over Figure 4.3 reveals that there is cross-isobaric flow in the north-central and northwest portions of the map. According to the geostrophic wind balance, since Figure 4.3 is determined by the geostrophic wind field (Figure 4.2) the winds should be parallel to the isobars. A number of sample calculations were accomplished to determine any errors in the computer result. No

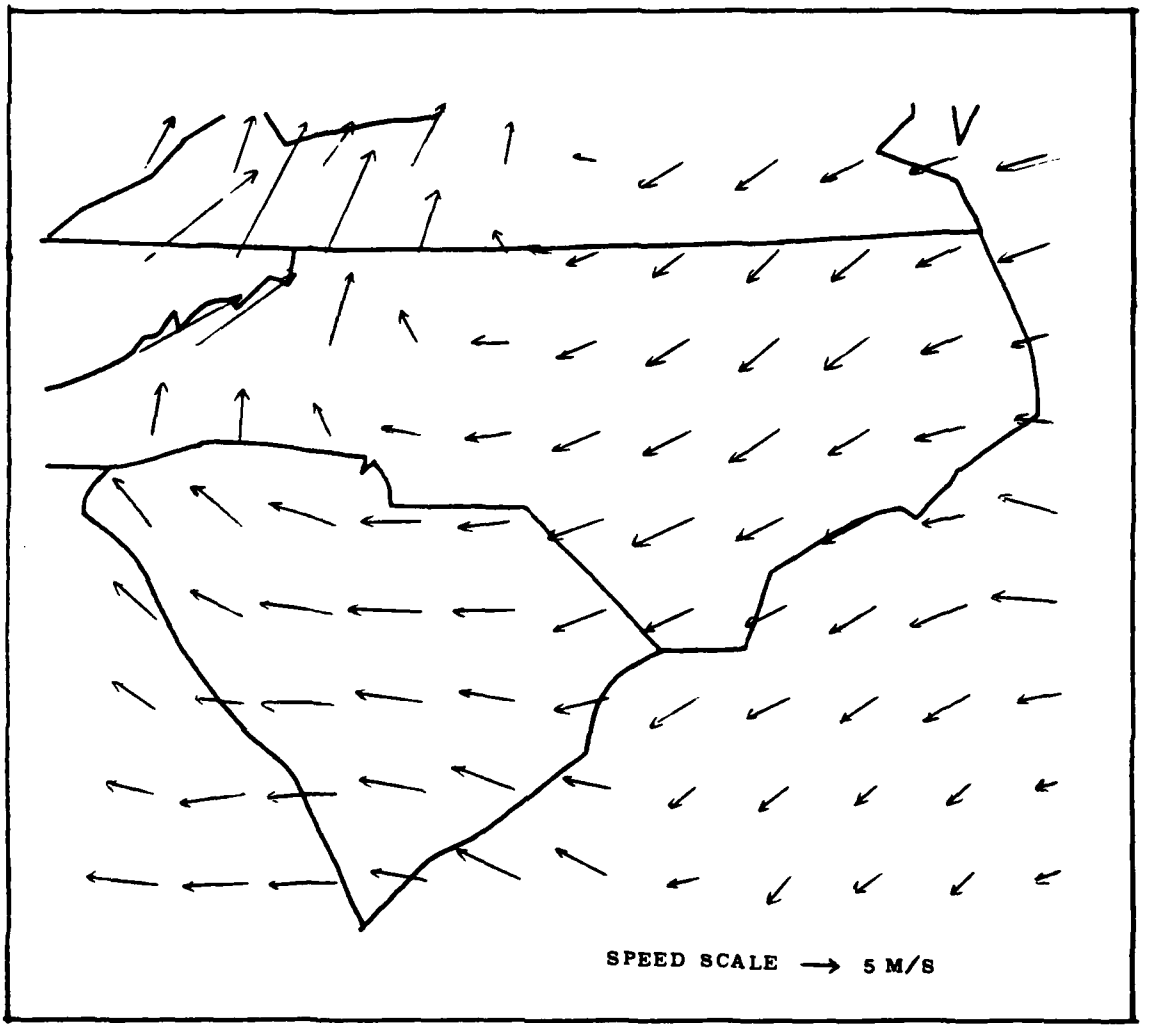

Figure 4.5. Geostrophic wind field calculated using the sea-level pressures for 1200 UTC 25 January 1986.

problems were found, so it would appear that, in the relaxation process, the forcing function defined by the geostrophic wind field is attempting to force the pressure field to conform as is expected, but the boundary conditions imposed on the pressure field are not allowing the pressure field to conform completely. Indeed, in comparing the two pressure fields (Figures 4.3 and 4.4) there is a slight westward shift

in the ridge axis in the surface pressure field suggesting the surface pressure field is attempting to conform to the geostrophic wind balance. A further complication in this case is that the mountains are located along the boundary adding the effect of the mountains to the effect of the boundary conditions. In the Pielke and Cram (1987) study a much larger area was used and there was evidence of cross-isobaric flow towards the boundary of the area. Therefore, had a larger area been employed in this research, the pressure field could be expected to conform more totally to the geostrophic wind field.

The final item to address in this section is whether the method for calculating geostrophic winds described in this section produces less of an ageostrophic component when compared to the observed wind field than the geostrophic wind calculated with the sea-level pressures. Figure 4.6 shows the wind vectors of the observed winds (o), the surface geostrophic winds from Figure 4.2 (SG), and the sea-level geostrophic winds from Figure 4.5 (G) for selected points. From Figure 4.6, a significant improvement can be seen in SG over G in the western Piedmont. The surface geostrophic winds are much closer to the observed winds than the geostrophic as was hoped. However, over the rest of the area, there is a slight improvement in direction of SG over G, but not much improvement in the speed. The observed winds are still ageostrophic, but SG seems to be a better representation of the observed winds than G.

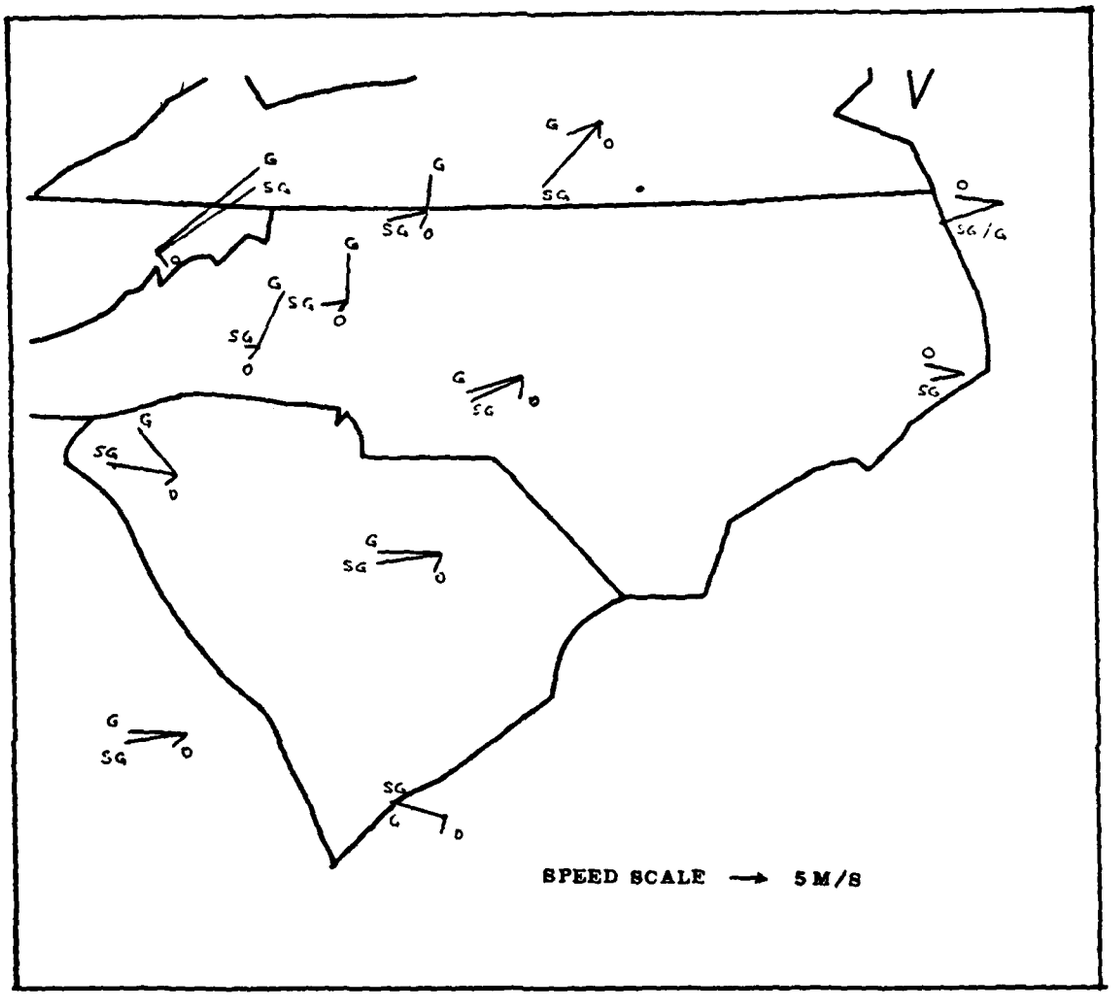

Figure 4.6. Plot of wind vectors of the observed winds (O), surface geostrophic winds (SG), and the sea-level geostrophic winds (G) for selected points at 1200 UTC on 25 January 1986.

5. CONCLUSIONS

The basic objective of this research is to enable the pressure data recorded at the PAM II stations during GALE to be used in mesoscale analyses. This objective was to be met by first correcting the pressures and then reducing the corrected pressures to sea level.

Pressure corrections were found for each of the PAM II stations using the Barnes objective analysis scheme to interpolate an altimeter setting to the PAM II stations from the altimeter settings reported by the NWS stations. The Barnes analysis scheme was selected over direct one-to-one comparisons between the PAM II stations and their nearest NWS neighbor for two reasons. First, not every PAM II station was located near a NWS station. Second, the Barnes analysis was expected to be a better method because it incorporated data from several stations into the interpolated altimeter setting. However, for the thirteen cases included in the comparisons, a Chi-squared test showed that the Barnes analysis did not provide a statistically significant improvement over the direct one-to-one comparison, or buddy check.

The interpolated altimeter setting was compared to the altimeter setting calculated from the observed station pressure for each PAM II station to obtain an offset. The offsets from thirteen cases were averaged to obtain the pressure corrections for each station. The corrections were applied to the station pressure and the corrected pressures were reduced to sea level using the method described in the Manual of Barometry (1963). The analysis of the reduced PAM II pressures and the reported NWS pressures matched well with the NMC

analysis for two separate cases, suggesting that the pressure corrections are valid for the GALE period.

The procedure outlined in the Manual of Barometry (1963) does not lend itself easily to manipulation by a computer as two of the corrections to the mean virtual temperature involve the use of tables. The result is a procedure that takes a great deal of time to find sea-level pressure. An empirical formula for calculating the mean virtual temperature without entering tables was developed to allow a computer to calculate the sea-level pressure for each station. The sea-level pressures calculated from this empirical formula were within 0.3 mb of the pressures computed using the tables. So, to a first approximation, this formula can be used in calculating sea-level pressures.

While the first two objectives have been met, the sea-level reduction procedure still involves a number of assumptions in the lapse rate through a fictitious column of air which was shown in previous work to create errors in the sea-level pressure analysis. A final objective of this research is to study an alternate method of pressure reduction. This method produces a horizontal pressure field from observations on a sloping surface by first calculating the geostrophic wind components defined on a terrain-following coordinate system. In this system, the pressure gradient term in the geostrophic wind equation consists of a modified pressure gradient term plus a height gradient, or slope, term. From the geostrophic wind components, the corresponding horizontal pressure field is obtained through the use of a relaxation method.

The resulting surface pressure field (Figure 4.3) has the same general pattern as the sea-level pressure analysis (Figure 4.4), but there appears to be a stronger gradient in the surface pressure field over the mountains than the sea-level pressure analysis. During cold-air damming situations, a tighter packing of the isobars against the mountains would be expected as colder air is being dammed up against the mountains. The sea-level pressure values are about 1 to 2 mb stronger than those obtained from the surface pressure analysis. It would appear that the assumptions used in the standard sea-level pressure reduction method reduce the effect off the cold-air damming resulting in a weaker gradient over the mountains and lead to artificially higher pressure.

The surface geostrophic winds are not parallel to the surface pressure isobars as is expected. In the relaxation process, the forcing function defined by the geostrophic wind field attempts to create a pressure field so the winds are parallel to the isobars, but the boundary conditions imposed on the pressure field along with the mountains located at the western boundary may prevent the pressures from conforming completely. Using a larger area so the mountains are away from the boundary should produce the expected results.

The surface geostrophic winds calculated from equation (4.5) were expected to be an improvement over the geostrophic winds calculated using the sea-level pressures. The observed winds were expected to be less ageostrophic relative to the surface geostrophic winds than to the sea-level geostrophic winds. Figure 4.6 shows there to be a direction

improvement, but not much of a speed improvement over much of the area of interest; however, over the western Piedmont, where the winds are most ageostrophic, the surface geostrophic winds are much closer to the observed winds than the geostrophic winds. One reason there is not much improvement in the speed elsewhere might be that the observed winds were so light (around 5 m/s). Even so, it would appear that the method introduced by Pielke and Cram (1987) is a better representation of the surface geostrophic winds than using the sea-level pressures.

6. FUTURE RESEARCH

Further research is needed to continue to validate the pressure corrections derived in this research. This could be done by applying the pressure corrections to other cases during GALE. One such case would be the cyclogenesis that occurred on 13 March 1986. The pressure corrections could be applied to the 5-minute data to determine if the corrected pressure data permit the detection of an important, but weak and short-lived low-pressure center that developed in the PAM II region.

Other applications of these pressure corrections would be the study of mesoscale thunderstorm cases, such as the one depicted in Figures 3.2 and 3.3 to determine whether a trigger can be detected in the mesoscale pressure pattern. *Finding a trigger* to these storms would enable better prediction.

Future research could also be directed toward studying the empirical formula derived in Chapter 3 for reducing station pressure to sea-level in order to create a formula for outside the GALE region and GALE period.

More important than working on the empirical formula would be continued testing of the alternate method of pressure reduction introduced by Pielke and Cram (1987) in order to determine whether the method can be used outside the Great Plains. One such test could be on a stronger cold-air damming case than was presented in this research to determine if the method produces winds closer to the observed winds over a larger area.

In computing the $\tilde{\pi}$ field from the geostrophic wind, a much larger area needs to be employed to ensure the terrain feature is away from the boundary and the boundary conditions themselves do not interfere with the computation of the $\tilde{\pi}$ field in the area of interest; in this case the GALE region.

7. REFERENCES

Abbe, Cleveland and Winslow Upton, 1882: **Annual Report of the Chief Signal Officer of the Army**, Washington D. C., 1882, Appendix 61, pp 826-846.

Bellamy, J.C., 1945: The use of pressure altitude and altimeter corrections in meteorology. **Journal of Meteorology**, 2, 1-79.

Brock, F. V. and P.K. Govind: Portable Automated Mesonet in Operation. **Journal of Applied Meteorology**, 16, 299-310.

Davies-Jones, Robert, 1988: Notes and Correspondence "On the Formulation of Surface Geostrophic Streamfunction." **Monthly Weather Review**, 116, 1824-1826.

Dirks, R.A., J.P. Kuettner, and J.A. Moore, 1988: Genesis of Atlantic Lows Experiment (GALE): An overview. **Bull of Amer Meteor Soc**, Vol 69, No. 2,pp 148-160.

Ferrel, William, 1886: On reduction of barometric pressure to sea level and standard gravity. **Annual Report of the Chief Signal Officer of the Army**, Washington, D.C., 1887, Appendix 23, pp 221-234.

Genesis of Atlantic Lows Experiment (GALE) Experiment Design, 1985: Prepared by the GALE Project Office, Boulder, Colorado, In consultation with, and on the behalf of, the GALE Experimental Design Panel.

Phillips, N.A., 1957: A coordinate system having some special advantages for numerical forecasting. **Journal of Meteorology**, 14, 184-185.

Pielke, Roger A., 1984: **Mesoscale Meteorological Modeling**, Academic Press, 612 pp.

_____, and C. L. Martin, 1981: The derivation of a terrain-following coordinate system for use in a hydrostatic model. **Journal of Atmospheric Science**, 38, 1707-1713.

_____, M. Segal, R. T. McNider and Y. Mahrer, 1985: Derivation of slope flow equations using two different coordinate representations. **Journal of Atmospheric Science**, 42, 1102-1106.

Pielke Roger A., and Jennifer M. Cram, 1987: An alternate procedure for analyzing surface geostrophic winds and pressure over elevated terrain. **Weather and Forecasting, 2,** 229-236.

Pike, J. M., 1985: Field Calibration of humidity instruments in the natural atmosphere. **Proceedings, International Symposium on Moisture and Humidity,** Instrum. Society of America, Washington DC, 111-119.

Sangster, Wayne E., 1960: A method of representing the horizontal pressure force without reduction of station pressures to sea level. **Journal of Meteorology, 17,** 166-176.

_____, 1987: An improved technique for computing the Horizontal Pressure-Gradient force at the Earth's surface. **Monthly Weather Review, 115,** 1358-1369.

Wade, Charles G., 1987: A quality control program for surface mesometeorological data. **Journal of Atmospheric and Oceanic Technology, Vol 4, No. 3,** 435-453.

Walpole, Ronald E. and Raymond H. Myers, 1978: **Probability and Statistics for Engineers and Scientists,** Macmillan, New York.

APPENDIX 8.1

EARLY METHODS OF SEA-LEVEL PRESSURE REDUCTION

The first method employed by the Weather Service was used from 1870 to mid-1881 and employed Guyot's Table XIX (Bigelow, 1900). This table provided the height, in feet, of a column of air corresponding to 0.10 in of mercury at different temperatures and elevations. The procedure was to increase the temperature of the higher elevation station to that of a lower station by using a standard lapse rate. Entering the table, one then could obtain the number of feet per 0.10 in mercury for each station. Next, one found the mean of these two heights and divided the elevation difference by this mean to obtain the correction to be added to the pressure of the higher elevation station (Bigelow, 1900).

This procedure was found to have involved two procedures which greatly exaggerated the diurnal variation of the isobars making them almost useless for forecasting (Bigelow, 1900). The first problem was that the temperature argument was taken as the reported surface temperature at the hour of observation rather than for a time average for the plateau column. Thus, the whole air column was considered subject to a diurnal range of temperatures which in fact is only characteristic of the air near the surface. The second problem was that Table XIX was only entered once to get the mean reduction number instead of twice; once to reduce the higher station to the elevation of

the lower station and once to reduce the lower station to sea level (Bigelow, 1900).

In an effort to eliminate the problems encountered using Guyot's tables, the Weather Service adopted a method that employed monthly constants for the reduction of pressure developed by Professors Abbe and Upton (1882). The Abbe-Upton method took three steps in determining the observed station temperature. The first was to compute the latitudinal average temperature at sea level. The second step was to calculate an average lapse rate for a given latitude. The final step was to calculate the variation of lapse rate along a given latitude (Abbe and Upton, 1882). The values of the temperature and lapse rate were used to calculate a mean monthly temperature of the station (Abbe and Upton, 1882). This mean monthly temperature was then used in Upton's formula for pressure reduction.

Three problems were soon found with this method. The first was that the sea level reduction of pressure ought to involve two other corrections, one depending on the deviation of pressure from the mean and the other depending on the deviation of temperature from the mean. These deviations occur almost constantly and must be taken into consideration, but are not considered when using monthly constants. The second problem was that Upton's computed lapse rates were greater in the winter than summer, whereas actual observations showed them to be greater in the summer. The final problem is that the method did not produce useful pressure fields (Bigelow, 1900).

As a result of the failure of the monthly constants, William

Ferrel was commissioned by the Weather Service to develop a new method for the reduction of pressures. Ferrel (1886) made four improvements to the earlier methods. The first was the substitution in the reduction procedure of the mean diurnal temperature instead of the temperature at the hour of observation. The second improvement was the introduction of a mean lapse rate to increase the surface temperature as an argument to the mean temperature of the air column. Ferrel (1886) adopted a lapse rate of 1°F per 600 feet and applied it for half the elevation of the station. The third improvement was the introduction of a thermal pressure term which Ferrel defined as CAH; where C is a constant with a value of 0.00105 in/°Fft, A is the departure of the temperature from the normal, and H is the station elevation in feet (Ferrel, 1886). The last improvement was the introduction of a plateau correction. Ferrel found that all the reduced pressures for all high stations were too great in January as a result of using temperatures that were too cold, and too low in July as a result of using temperatures that were too warm. It was necessary to apply some correction to the reductions for these extremes. The correction was determined on the principle that the differences of the reduced pressures of the high stations in January and July should not be greater than those of the low-level stations, which Ferrel found to be 0.15 in. (Ferrel, 1886). The plateau correction Ferrel developed is defined as follows:

$$a = c + \Delta H \qquad (1.1)$$

with a = correction of pressure reduced to sea level (in).

c = average departure of pressure at sea level from the normal annual pressure (in).

CAH = is the thermal pressure term as defined above.

Ferrel assumed c to be a constant and equal to 0.073 in. However, Bigelow (1900) reported that c is not a constant, but has an annual range from +0.073 to −0.073. The value should be calculated monthly as well as for the mean for January and July (Bigelow (1900).

In his report of 1900, Bigelow introduced improvements to Ferrel's techniques by adopting a variable lapse rate for the fictitious air column and a humidity correction as a function of the surface temperature, and by redefining the temperature argument.

Bigelow believed that the assumed lapse rate in the fictitious air column should vary with the location of the station, the height above sea level, and the month. If the assumed lapse rate is allowed to vary in an appropriate manner with the station temperature argument depending on the station, it would not be necessary to regard the monthly temperature as anomalous (Manual of Barometry, 1963).

In his method for dealing with the humidity term, he took the vapor pressure at the surface and employed the following formula to compute an average vapor pressure of the column:

$$e = e_0^{-h/6317} \qquad (1.2)$$

where h is the height in meters, e_0 is the vapor pressure at sea level, and e is the vapor pressure at height, h (Bigelow, 1900). Bigelow

added a correction to the above formula for abnormal conditions. This formula is:

$$e = e_0^{-h/(6317 \pm a)} \qquad (1.3)$$

Finally, Bigelow defined the station temperature argument as the average of the current observed temperature and the observed temperature twelve hours previously (Manual of Barometry, 1963).

The Weather Service adopted a method that includes the work of Ferrel and Bigelow. The pressure reduction is accomplished using the hypsometric equation with the temperature replaced by the mean virtual temperature of the air column. The calculation of the mean virtual temperature includes the temperature argument defined by Bigelow, a standard lapse rate correction, a humidity correction first introduced by Bigelow, and a plateau correction developed by Ferrel (Manual of Barometry, 1963).

APPENDIX 8.2

This table presents the PAM II station elevations used in this research. Elevations are in meters.

Station	Elevation	Station	Elevation
01	2	26	271
02	18	27	373
03	50	28	722
04	93	29	764
05	142	30	2
06	3	31	11
07	29	32	56
08	87	33	114
09	163	34	166
10	130	35	8
11	3	36	13
12	15	37	35
13	41	38	72
14	80	39	135
15	186	40	2
16	6	41	2
17	15	42	8
18	27	43	41
19	105	44	88
20	151	45	2
21	4	46	1
22	19	47	1
23	46	48	1
24	138	49	3
25	191	50	23

APPENDIX 8.3

This table presents the differences (in mb) found for each station for each case used in the Barnes objective analysis. "*****" indicates data missing for PAM station.

Station	1/20	1/24	2/02	2/11	2/13	2/14	2/23	2/25	2/27	3/01	3/06	3/08	3/13
01	0.36	0.45	0.44	0.43	0.35	0.16	-0.17	0.30	0.66	0.12	-0.01	0.39	0.08
02	0.32	0.93	0.25	0.38	1.01	0.91	0.86	0.83	0.33	0.45	-0.17	0.79	0.47
03	-1.15	-1.28	-1.22	-1.31	-0.92	-0.95	-1.23	-0.86	-1.92	-1.44	-1.47	-0.86	-0.93
04	0.44	-0.49	0.05	0.50	0.01	-0.17	0.24	-0.22	0.24	-0.49	-0.03	-0.10	-0.70
05	1.00	0.49	0.44	1.48	1.30	0.73	1.73	0.94	1.68	1.06	1.16	1.34	0.70
06	0.08	-0.63	2.36	0.85	0.99	0.63	0.40	0.79	1.08	0.31	0.09	0.13	0.32
07	1.17	0.68	1.05	0.51	1.68	1.85	1.99	1.99	1.03	1.48	1.11	1.87	1.28
08	0.77	0.36	0.78	0.47	0.79	1.01	0.78	0.86	-0.15	1.05	0.68	0.61	1.24
09	-1.18	-1.38	-0.41	-0.31	-1.26	-1.24	-0.04	-1.07	-0.56	-1.21	-1.15	-1.06	-0.57
10	-1.56	-1.91	-1.59	-1.44	-1.22	-1.52	-1.04	-1.07	-1.86	-1.48	-2.91	-2.72	-3.51
11	0	-0.92	-0.07	-0.63	-0.48	-0.26	-0.74	0.44	0.06	0.34	-0.19	0.78	0.11
12	0.32	-0.29	0.64	0.23	0.28	0.52	0.51	0.91	0.34	0.68	*****	*****	-1.27
13	0.38	0.96	0.72	0.14	1.33	1.17	0.98	0.76	0.34	0.56	0.41	1.10	0.49
14	-0.49	-0.15	-0.02	-0.16	0.13	0.06	0.11	-0.11	-0.15	-0.31	-0.15	0.53	-0.47
15	-0.09	-0.73	-0.13	-0.03	-0.29	-0.29	0.18	0.04	-0.60	-0.34	-0.53	-0.19	-1.14
16	-0.77	-0.93	-0.51	-0.82	-0.60	-0.25	-0.73	-0.84	-0.20	-0.92	-0.42	-0.06	-0.45
17	0.76	-0.26	0.58	0.21	0.24	0.10	-0.09	0.84	0.89	0.48	0.33	-0.05	0.32
18	0.16	0.21	0.19	0.10	0.35	0.09	0.60	0.53	-0.23	0.50	-0.16	0.43	-0.55
19	-0.92	-1.04	-1.05	-1.28	-1.12	-1.23	-0.48	-0.96	-1.18	-1.14	-0.90	-0.91	-1.12
20	1.57	0.95	0.60	1.79	1.26	1.15	1.49	1.14	1.15	1.71	0.14	1.57	0.70
21	1.80	1.22	1.79	2.68	1.80	2.30	1.95	2.36	2.26	1.58	2.30	2.89	2.21
22	1.43	1.16	1.71	1.33	1.71	1.23	1.78	1.66	1.91	1.49	1.58	1.66	1.73
23	0.04	0.06	0.33	0.51	0.51	-0.49	0.48	0.48	-0.23	0.59	-0.31	-0.10	-0.31
24	-0.34	*****	2.01	1.81	*****	1.59	*****	2.37	1.95	2.43	2.09	*****	-0.07
25	0.92	0.32	1.01	1.31	0.50	0.29	1.39	1.28	1.22	1.13	1.22	0.77	1.01

APPENDIX 8.3 (continued)

This is the continuation of the differences (in mb) found for each station for each case used in the Barnes objective analysis. "*****" indicates data missing for PAM station.

Station	1/20	1/24	2/02	2/11	2/13	2/14	2/23	2/25	2/27	3/01	3/06	3/08	3/13
26	0.72	1.25	0.80	-0.52	-0.01	-0.35	-1.22	-0.66	-0.31	0.35	0.08	1.64	0.15
27	0.39	1.35	0.73	0.58	1.07	1.32	0.49	0.53	-0.03	0.45	1.04	0.65	0.68
28	-1.56	-1.40	-0.11	-1.74	-2.32	-1.63	-1.62	-1.67	-1.45	-2.95	-1.23	-2.11	0.17
29	-0.16	-1.63	-1.05	-1.01	-1.25	-1.56	-1.01	-1.01	-1.36	-2.46	-1.86	-1.68	-1.68
30	-0.22	0.26	-0.24	-0.46	0.40	-0.58	-0.62	0.56	-0.22	0.44	-0.19	0.60	-0.63
31	-0.06	-0.02	-0.10	-0.96	0.71	0.66	-0.50	0.43	-0.48	0.44	-0.25	-0.20	-0.19
32	2.40	1.77	3.71	3.62	2.33	2.01	2.30	2.36	2.76	2.18	2.06	1.93	3.14
33	-0.33	0.04	-0.07	0.02	0.49	0.32	0.44	0.43	-0.19	0.09	-0.12	0.35	0.43
34	0.23	-0.21	-0.14	-0.13	-0.32	-0.51	-0.05	-0.13	-0.36	-0.37	-0.43	-0.65	0.21
35	1.99	1.98	2.17	1.59	3.03	1.56	2.50	2.69	3.23	2.70	2.96	2.89	2.70
36	-0.28	0.36	0.55	-0.07	1.19	-0.30	0.46	0.33	0.60	0.33	0.23	0.03	0.04
37	-0.08	0.08	0.27	-0.11	0.62	-0.79	0.10	0.50	0.35	0.16	0	-0.06	-0.10
38	-0.69	0.22	-0.70	-0.31	0.13	0.21	0.02	0.28	0.15	0.31	-0.92	0.54	-0.18
39	-0.98	-0.76	-0.77	-0.39	-0.86	-0.29	0.06	-0.63	-0.50	*****	-0.77	0.01	-0.27
40	-0.14	-0.01	-0.37	-0.71	0.05	-0.22	-0.11	0.09	0.01	0.39	0.04	-0.58	-0.32
41	1.54	2.05	1.51	1.90	2.88	1.44	1.83	2.02	1.71	1.82	2.15	2.07	1.77
42	-0.14	0.05	0.15	0.53	0.47	-0.17	0.32	0.46	0.22	0.08	-0.05	0.19	-0.01
43	-1.22	*****	-0.74	0.02	-0.43	-0.67	-0.01	-0.21	-0.65	-1.03	-1.74	-0.07	-0.67
44	-0.86	0.44	-0.49	0.79	0.45	0.33	0.54	1.04	0.23	0.23	-1.12	0.21	0.24
45	-0.40	-0.21	-0.76	-0.76	-0.62	-1.44	-1.22	-0.94	-0.83	-0.14	-0.29	-1.47	-1.37
46	0.35	0.53	0.60	0.72	0.65	-0.33	-0.01	-0.21	-0.23	-0.36	0.12	-0.53	-0.39
47	0.02	-0.15	0.03	0.46	0.02	-0.10	-0.29	-0.33	0.33	-0.08	0.24	0.34	-0.04
48	0.30	0.26	0.21	0.30	0.21	-0.11	-0.44	-0.30	-0.51	0.13	-0.08	0	-0.49
49	-0.19	-0.33	-0.26	-1.12	-0.53	-0.73	-0.84	-1.00	-0.83	-0.85	-0.87	-0.68	-1.38
50	-0.53	-0.30	-0.28	0.55	-0.10	-0.30	0.22	0.39	-0.46	-0.91	-1.14	0.14	-0.77